Pre-pub. on line: www.geojournals.cn/georev

# 南秦岭武当山十堰地区中生代镁铁质岩石成因与构造意义

## ——岩石地球化学、锆石U-Pb年龄和Hf同位素制约

王嘉玮[1,2)],王刚[2)],王宗起[2)],武昱东[2)],王东升[2)],王坤明[2)]

1)中国地质大学(北京),北京,100083;

2)中国地质科学院矿产资源研究所,自然资源部成矿作用与资源评价重点实验室,北京,100037

**内容提要**:南秦岭的北大巴山-武当山-十堰-随州一带发育大规模的镁铁质岩墙群,其岩石学成因为地质学家所广泛关注。本文对其中的武当山十堰地区黄龙-方滩一带发育的辉长岩体开展了全岩地球化学、SHRIMP锆石U-Pb年龄以及LA-MC-ICP-MS锆石Hf同位素组成研究。结果表明,辉长岩形成于晚三叠世(221.2±2.5 Ma);岩石地球化学组成显示辉长岩为亚碱性拉斑玄武岩系列,轻稀土富集重稀土亏损,其平滑右倾的稀土配分模式与E-MORB相似;中等Ti、Zr、Hf、Nb含量,亏损Rb、Sr等大离子亲石元素,以及结晶年龄锆石的$\varepsilon_{Hf}(t)$值在-13.5至-6.18之间,表明岩石具有古老的两阶段Hf模式年龄(2103~1640 Ma)。综合分析表明:该套辉长岩岩浆为尖晶石二辉橄榄岩低压、中等程度部分熔融形成,并且其源区为亏损地幔与富集地幔组分混合成因;结合区域构造演化的相关资料,认为该套E-MORB性质辉长岩形成于类似汇聚边缘的构造环境,可能为受勉略洋壳俯冲影响,为俯冲-碰撞造山阶段产物。

**关键词**:岩石成因;中生代;辉长岩;武当山;南秦岭

南秦岭北大巴山-武当山-十堰-随州一带近千千米造山带中发育大规模的镁铁质岩墙群或岩脉(周鼎武等,1997;张成立等,2002;胡健民等,2004;薛怀民等,2011)。综合分析前人研究发现,该区镁铁质岩石主要集中在:① 新元古代(850~610 Ma)拉斑玄武岩系列和碱性玄武岩系列,部分代表了岛弧-弧后伸展构造环境(苏文等,2013; Xu Yang et al., 2016; 刘嘉威等,2018),部分代表了地幔柱-裂谷环境(周鼎武等,1998,1999; 薛怀民等,2011; Wang Lijuan et al., 2013; Zhu Xiyan et al., 2015; Li Qiwei et al., 2016);② 古生代(470~400 Ma)碱性玄武岩系列具有板内洋岛玄武岩特征,是区域伸展构造背景下产物,但伸展构造机制存在幔源岩浆底侵(胡健民等,2002,2003,2004)、大陆裂谷(王存智等,2009;邹先武等,2011;Nie Hu et al., 2016)和弧后伸展等不同认识(王坤明等,2014; Wang Kunming et al., 2015;许光等,2018);③ 区域内仅有少量中生代的报道(220 Ma),前人认为其代表了印支期勉略洋闭合后由碰撞挤压转换为伸展环境(Nie Hu et al., 2016)。综上可见,南秦岭造山带发育多期次且构造背景复杂的镁铁质岩浆,对武当-随州地区部分或整体发育的镁铁质岩的产出状态,仍存在侵入(周鼎武等,1998;胡健民等,2004;薛怀民等,2011)和构造侵位(王荃等,2010;王宗起等[4])等不同认识。本文对武当山十堰黄龙-方滩地区发育的侵入状辉长岩体进行了详细的岩石地球化学、锆石U-Pb年代学和Hf同位素研究,阐明其形成时代和岩石成因,从而为进一步认识区域中生代基性岩墙特征和理解区域构造演化提供新的证据。

## 1 区域地质背景

武当山是南秦岭造山带的重要组成部分(图1a),主要发育武当群变沉积岩和基性、中酸性变火山岩组,其上为耀岭河群变玄武质火山岩(熔岩、火

注:本文为国家重点研发计划(编号:2016YFC0600202)和中国地质科学院基本科研业务费项目(编号:YK1701)的成果。

收稿日期:2021-01-15;改回日期:2021-03-25;网络首发:2021-05-20;责任编辑:黄道袤,刘志强。Doi: 10.16509/j.georeview.2021.03.257

作者简介:王嘉玮,男,1989年生,博士,助理研究员;主要从事岩石学、构造地质学和成矿作用研究;Email:wangjiawei0824@163.com。通讯作者:王刚,男,1984年生,博士,助理研究员;主要从事构造与成矿作用研究;Email:wanggang0315@126.com。

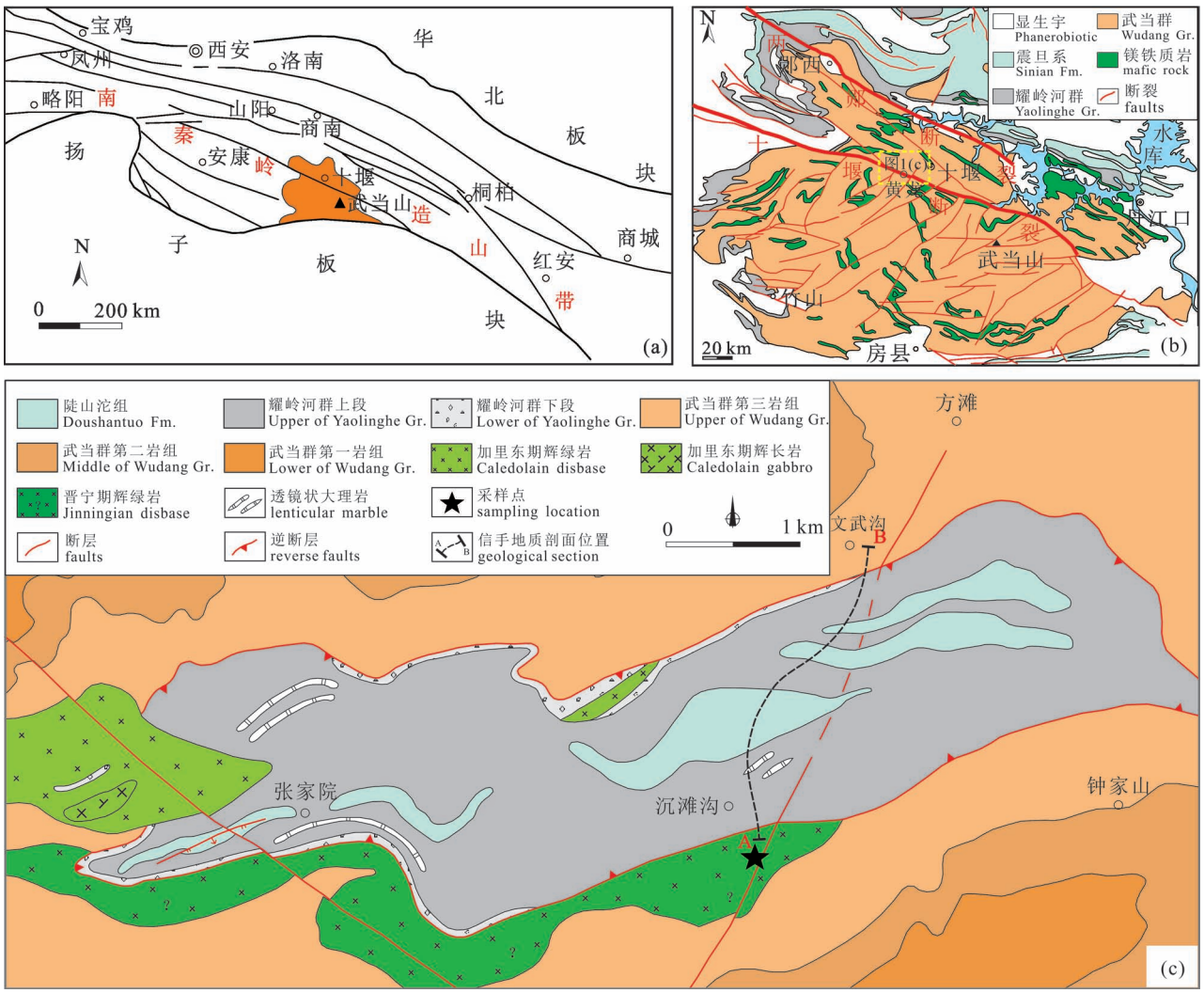


图 1 武当-十堰地区大地构造位置(a)和武当地区地质简图(b,据凌文黎等,2007)以及黄龙-方滩一带地质简图(c,据湖北十堰黄龙-方滩地区 1∶5 万地质简图,1985)

Fig. 1 Location of Wudang Mountain in Qinling-Dabie Orogen(a), geological map of Wudang Mountain(b; modified from Ling Wenli et al., 2007) and geological map of the Huanglong-Fangtan area(c; after 1∶50000 geological map of the Huanglong-Fangtan area, Shiyan City of Hubei Province,1985)

山碎屑岩或凝灰岩)夹少量变酸性火山岩和变泥质岩基性火山-沉积岩(陈晋镳等,1991;付建明等,1999;蔡志勇等,2006;祝禧艳等,2008;张永清等,2013),二者接触关系存在整合和构造拼合接触等不同认识(陈晋镳等,1991;胡健民等,1995;祝禧艳等,2008)。震旦系发育在武当山周缘,为陡山沱组和灯影组次深海相沉积岩。此外,区域内还发育新元古代、古生代及中生代多期次岩浆活动,以镁铁质-超镁铁质岩为主,并有少量花岗质岩石出露(周鼎武等,1997;胡健民等,2004;凌文黎等,2007;苏文等,2013;Zhu Xiyan et al., 2015;Li Qiwei et al., 2016;Nie Hu et al., 2016;Wang Ruirui et al., 2016)。区域上发育北西向和北东向构造,武当地块被北部的两郧断裂和南部的十堰断裂(图 1b)分为北部、南部和中部 3 个不同的构造区段(赵国春等,2003;胡建民等,2004),两条断裂总体呈北西西向展布,断面北倾,它们之间发育武当群、耀岭河群以及镁铁质的辉绿岩和辉长岩(周鼎武等,1999;胡健民等,2003;Wang Lijuan et al., 2013),少量超镁铁质的辉石岩(湖北省地质矿产局区域地质矿产调查所[1];湖北省地质调查院[3])和花岗质侵入岩(Wang Ruirui et al., 2016;图 1b)。研究区黄龙-方滩一带位于十堰断裂北侧,构造变形强烈,前人通过地层对比认为该地区物质组成与武当地块整体一

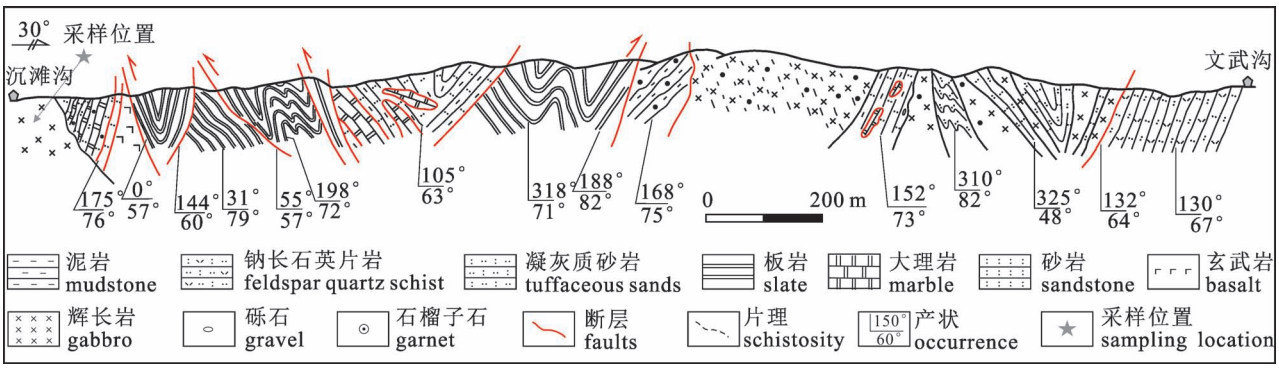


图 2 湖北十堰黄龙沉滩沟-文武沟信手剖面图(据王刚等,2018)

Fig. 2 Geological section from Chentangou to Wenwugou of Huanglong area, Shiyan city of Hubei Province (from Wang Gang et al., 2018&)

致,主要由武当群、耀岭河群和局部出露的陡山沱组等前寒武系有序地层及少量晋宁期和加里东期镁铁质岩组成(湖北省地质矿产局区域地质矿产调查所❷,图 1c)。王刚等(2018)报道了该地区原划定的前寒武纪岩石地层中发现晚古生代沉积组合与火山活动物质的存在,且为海相沉积特征,后续又报道该地区发育中二叠世 E-MORB 型玄武岩块体,为洋中脊或附近海山环境(王刚等,2019)。此外,获得了大量不同时代年代学证据,并结合野外构造解析和室内研究提出黄龙-方滩地区是包含了新元古代-古生代-中生代等若干不同时代的物质组成的混杂岩带(王宗起等❹)。因此,研究区内前人划归的前寒武纪地层以及发育的镁铁质岩的时代等应予以重新认识和研究。

## 2　样品和测试方法

### 2.1　样品

通过对武当十堰黄龙地区沉滩沟-文武沟一带进行路线剖面调查(图 1c)、样品采集和室内测试分析,在研究区识别出一套玄武岩、灰岩(大理岩)块体,与碳硅质砂板岩、凝灰质砂岩和大理岩互层产出,并呈岩片状包裹于碎屑砂岩、变凝灰质砂岩(片岩)和变质泥岩(含石榴石二云母片岩)等岩石中(图 2;王刚等,2018,2019)。本文辉长岩体规模较大,原 1∶5 万地质图中将该部分岩体划归为晋宁期辉绿岩体(湖北省地质矿产局区域地质矿产调查所❶),图岩体东西向延伸近 5 km,宽度 100~200 m,地质图中岩体北侧与地层呈断层接触,野外实际考察中发现岩体呈侵入状切层产出(图 3a),但未见明显的冷凝边和烘烤边,岩体具有一定岩相变化,自两侧向中部表现为中细粒结构辉绿辉长岩逐渐过渡为中粗粒似斑状结构辉长岩,本文样品采集于岩体中部辉长岩(图 3b),采样点经纬度为:N32° 42' 51.43",E110°35' 22.81"。

镜下观察得出,所采辉长岩为辉长辉绿结构(图 3c),局部发育嵌晶结构(图 3d)。主要矿物为单斜辉石(35%~37%)、斜长石(45%~50%)、角闪石(~5%)、金属矿物(钛铁矿、磁铁矿;~8%);副矿物磷灰石。单斜辉石呈自形-半自形晶产出,粒径为 1~1.5 mm,个别颗粒绿泥石化;斜长石多呈半自形窄板状晶体产出,粒径为 1~2 mm,个别颗粒钠长石化。钛铁矿呈半自形粒状晶体(图 3c),磷灰石呈细小的柱状体(图 3d)。

### 2.2　测试方法

样品磨片、碎样和锆石挑选工作由河北省区域地质矿产调查研究所实验室完成。全岩主微量及稀土元素测试由中国地质科学院国家地质实验测试中心完成。主量元素采用 XRF 方法测试,FeO 用湿化学法单独分析;微量元素和稀土元素采用等离子质谱仪(PE300D)测试。其中 $Fe_2O_3$、$P_2O_5$、$TiO_2$、MnO 的检测准确度为 10%,其余数据检测准确度为 1%;微量和稀土元素含量大于 $10\times10^{-6}$ 的元素分析相对误差小于 5%,小于 $10\times10^{-6}$ 的元素分析相对误差小于 10%。用常规方法将岩石破碎,经磁法和密度分选后,经淘洗烘干并在双目镜下挑选锆石,锆石样品的制靶和阴极发光图像工作以及锆石 U-Pb 定年测试分析在中国地质科学院地质研究所北京离子探针中心完成,详细实验测试过程可参见宋彪等(2002)。锆石 U-Pb 年龄测定前,依据透反射图像和阴极发光图像分析,对锆石样品随机圈定裂隙和

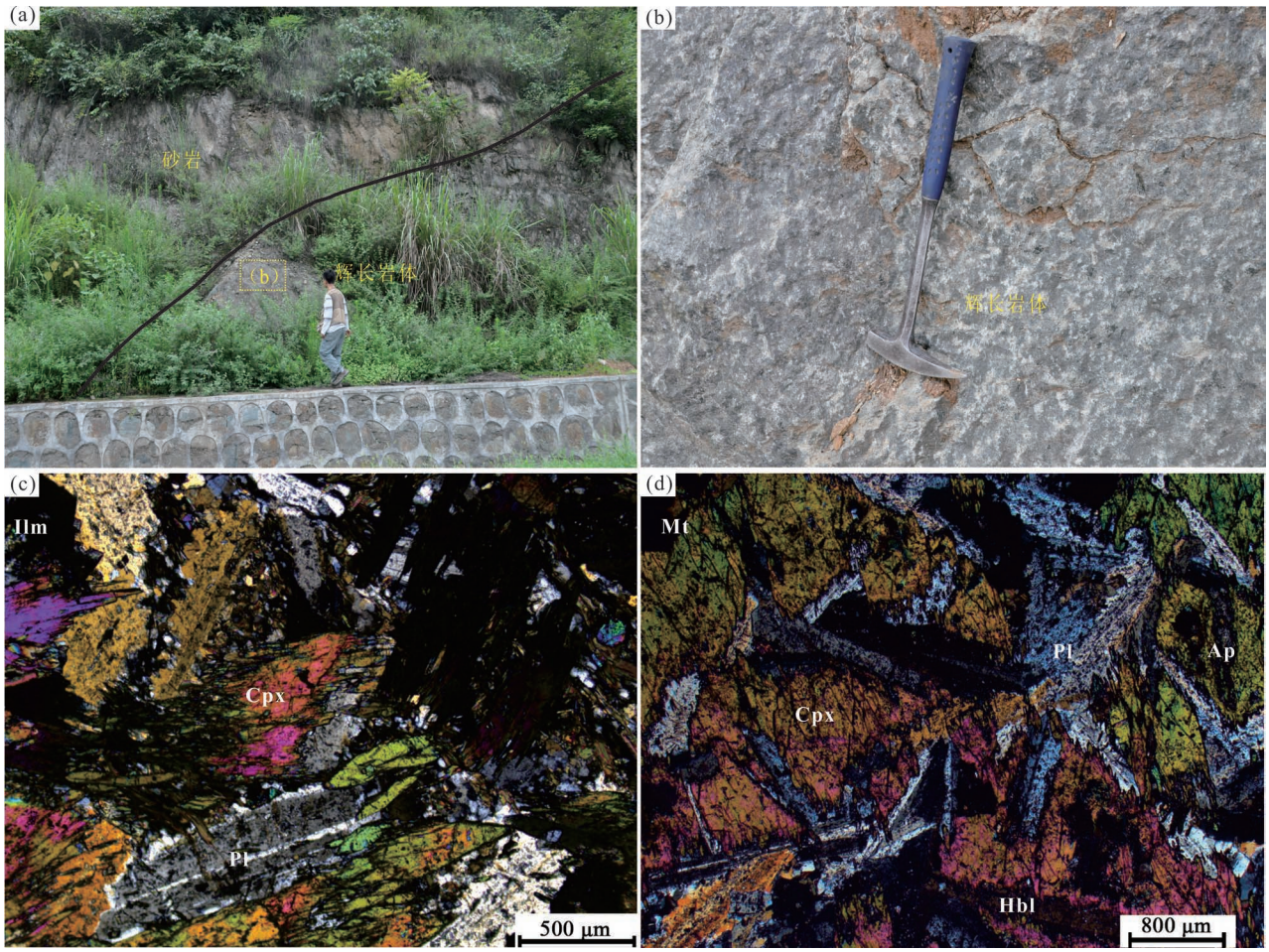


图 3 十堰黄龙沉滩沟辉长岩露头和显微照片

Fig. 3 Outcrops and microscopic texture of mafic rocks in Huanglong-Chentangou area, Shiyan city

Cpx-单斜辉石; Pl-斜长石; Ap-磷灰石; Mt-磁铁矿; Ilm-钛铁矿;

Cpx-Clinopyroxene; Pl-Plagioclase; Ap-Apatite; Mt-Magnetite; Ilm-Ilmenite

包裹体不发育的颗粒。SHRIMP 数据普通 Pb 由实测$^{204}$Pb 校正,锆石年龄谐和图等由 Isoplot 3.0 程序完成(Ludwig,2003)。锆石 Hf 同位素测试分析在中国地质科学院矿产资源研究所同位素实验室完成,所测点位与测年点位一致,使用仪器为 Finnigan Neptune 型多接收等离子质谱仪和 Newwave UP 213 激光剥蚀系统,采用 GJ1 作为外标,仪器运行条件和详细实验测试过程可参见侯可军等(2009)。

## 3 测试结果

### 3.1 锆石 U-Pb 年龄

辉长岩样品中的锆石颗粒呈无色透明自形、半自形结构,CL 图像显示大部分呈灰黑色均质结构,部分发育生长振荡环带。锆石粒径为 40~180 μm,长短轴比值为 4∶1~2∶1。本文对 16 颗单颗粒锆石进行 SHRIMP 方法测试,数据见表 1。获得了 8 颗时代分散于古元古代(2485 Ma)、中元古代(1019 Ma)、新元古代(825 Ma,747 Ma,639 Ma,625 Ma)、古生代(528 Ma,427 Ma)等的继承或捕获锆石年龄,其余 8 颗锆石年龄集中在 215~233 Ma(图 4a、b)。锆石形态和 Th/U 值(0.16~0.82,均大于 0.1)表明这些锆石为岩浆成因,其中 6 颗锆石加权平均年龄为 221.2±2.5 Ma(MSWD = 3.2),代表了辉长岩结晶年龄。

### 3.2 岩石地球化学组成

本次选取了 5 件样品进行岩石地球化学测试分析,测试数据见表格 2。样品 $SiO_2$ 变化范围介于 43.71%~49.99%(均值 47.78%);$TiO_2$ 含量介于 1.27%~2.65%(均值 1.84%);其余主要元素含量的变化范围均不大,其中 $Al_2O_3$ 和 $Fe_2O_3^T$ 分别介于

**表 1 湖北十堰黄龙-方滩地区辉长岩 SHRIMP 锆石 U-Pb 测年数据**

**Table 1 SHRIMP zircon U-Pb isotopic data for gabbro sample from the Huanglong-Fangtan area, Shiyan City of Hubei Province**

| 测试点号 | 元素含量($\times10^{-6}$) | | | Th/U | 同位素比值 | | | | | | 误差相关系数 | 同位素年龄(Ma) | | | | 不和谐度(%) |
|---|---|---|---|---|---|---|---|---|---|---|---|---|---|---|---|---|
| | $^{206}Pb^*$ | Th | U | | $n(^{207}Pb^*)/n(^{206}Pb)$ | | $n(^{207}Pb^*)/n(^{235}U)$ | | $n(^{206}Pb^*)/n(^{238}U)$ | | | $n(^{206}Pb)/n(^{238}U)$ | | $n(^{207}Pb)/n(^{206}Pb)$ | | |
| | | | | | 测值 | ±% | 测值 | ±% | 测值 | ±% | | 测值 | 1σ | 测值 | 1σ | |
| SY112-01 | 22.4 | 718 | 250 | 2.97 | 0.05870 | 2 | 0.8430 | 2.1 | 0.1042 | 0.81 | 0.379 | 639 | ±5.0 | 556 | ±43 | -15 |
| SY112-02 | 56.3 | 891 | 1827 | 0.5 | 0.05112 | 1.3 | 0.2528 | 2.1 | 0.03586 | 1.6 | 0.777 | 227 | ±3.7 | 246 | ±31 | 8 |
| SY112-03 | 83.2 | 176 | 564 | 0.32 | 0.07318 | 0.77 | 1.733 | 0.92 | 0.1717 | 0.50 | 0.542 | 1022 | ±4.7 | 1019 | ±16 | 0 |
| SY112-04 | 66.6 | 98 | 162 | 0.63 | 0.1628 | 0.57 | 10.74 | 1.5 | 0.4786 | 1.3 | 0.921 | 2521 | ±28 | 2485 | ±9.5 | -1 |
| SY112-05 | 9.39 | 124 | 318 | 0.4 | 0.04460 | 8.2 | 0.2090 | 8.2 | 0.03395 | 0.96 | 0.116 | 215 | ±2.0 | | | 376 |
| SY112-06 | 37.3 | 195 | 1240 | 0.16 | 0.05230 | 1.8 | 0.2529 | 1.8 | 0.03508 | 0.46 | 0.251 | 222 | ±1.0 | 298 | ±40 | 26 |
| SY112-07 | 49.7 | 1214 | 568 | 2.21 | 0.06076 | 1 | 0.8523 | 1.1 | 0.1017 | 0.47 | 0.417 | 625 | ±2.8 | 631 | ±22 | 1 |
| SY112-08 | 23.8 | 192 | 790 | 0.25 | 0.05167 | 1.7 | 0.2502 | 1.8 | 0.03511 | 0.49 | 0.273 | 223 | ±1.1 | 271 | ±39 | 18 |
| SY112-09 | 19 | 246 | 626 | 0.41 | 0.04939 | 1.9 | 0.2401 | 1.9 | 0.03525 | 0.53 | 0.277 | 223 | ±1.2 | 167 | ±43 | -34 |
| SY112-10 | 25 | 254 | 787 | 0.33 | 0.04870 | 2.5 | 0.2477 | 2.6 | 0.03686 | 0.56 | 0.215 | 233 | ±1.3 | 135 | ±59 | -73 |
| SY112-11 | 53.3 | 75 | 454 | 0.17 | 0.1060 | 2.2 | 1.994 | 2.4 | 0.1365 | 0.91 | 0.377 | 825 | ±7.0 | 1731 | ±41 | 52 |
| SY112-12 | 28.3 | 231 | 385 | 0.62 | 0.05860 | 1.8 | 0.6890 | 1.9 | 0.08528 | 0.63 | 0.333 | 528 | ±3.2 | 551 | ±39 | 4 |
| SY112-13 | 10.6 | 63 | 100 | 0.65 | 0.06590 | 4 | 1.116 | 4.2 | 0.1228 | 1.1 | 0.254 | 747 | ±7.4 | 803 | ±84 | 7 |
| SY112-14 | 43.8 | 100 | 742 | 0.14 | 0.05662 | 1.6 | 0.5350 | 1.7 | 0.06853 | 0.50 | 0.296 | 427 | ±2.1 | 477 | ±36 | 10 |
| SY112-15 | 12.5 | 333 | 420 | 0.82 | 0.05270 | 2.1 | 0.2523 | 2.2 | 0.03474 | 0.78 | 0.35 | 220 | ±1.7 | 314 | ±47 | 30 |
| SY112-16 | 29.9 | 190 | 1013 | 0.19 | 0.05180 | 2 | 0.2457 | 2.1 | 0.03440 | 0.45 | 0.218 | 218 | ±0.97 | 277 | ±46 | 21 |

注:$^{206}Pb^*$ 和 $^{206}Pb$ 分别表示放射性成因铅和普通铅;普通铅根据实测 $^{204}Pb$ 进行校正,误差为 1σ。

13.94%~15.32%(均值 14.7%)和 9.24%~16.21%(均值 12.90%);CaO 含量在 8.27%~11.35%(均值 9.66%);$Na_2O$ 含量介于 2.37%~4.03%(均值 3.34%);MgO 含量 6.03%~7.30%,$Mg^{\#}$ 值介于 42~61;全碱含量介于 2.67%~4.69%。在 TAS 分类图解中(图 5a),大部分样品都落在亚碱性系列辉长岩区域。在 10000 $Zr/TiO_2$-Nb/Y 分类图解上(图 5b),所有样品都落于亚碱性系列辉长岩区域。在 $K_2O$-$SiO_2$ 图解和 Y-Zr 图解上(图 6a、b)进一步划分为拉斑玄武岩系列。与 Nie Hu 等(2016)报道的武当山南部发育的中生代(~220 Ma)镁铁质岩具有相似的岩浆系列特征。

辉长岩样品 ∑REE 值介于 $54.4\times10^{-6}$~$111\times10^{-6}$,其中 ∑LREE 集中在 $43.2\times10^{-6}$~$91.7\times10^{-6}$,∑HREE 值介于 $11.2\times10^{-6}$~$19.7\times10^{-6}$;轻重稀土比值介于 3.77~4.65,$(La/Yb)_N$ = 3.47~4.85,所有样品均显示轻稀土富集重稀土亏损的特征;$(La/Sm)_N$ = 1.71~2.11,轻稀土轻微分异;$(Gd/Lu)_N$ = 1.66~1.95,说明重稀土亦轻微分异;在球粒陨石标准化的稀土分配模式图中大部分样品呈平坦微右斜模式,类似于 E-MORB 稀土配分曲线,轻重稀土分异程度低于 OIB 和土耳其地区造山带后碰撞阶段碱性玄武岩(图 7a)。样品 δEu = 0.95~1.18,平均为 1.01,Eu 异常不明显;样品 δCe = 1.04~1.05,平均为 1.05,无明显异常。Nie Hu 等(2016)报道的武当山南部发育的中生代镁铁质岩显示出 N-MORB 和 E-MORB 两种稀土配分曲线特征,三组样品从空间展布上看,自南向北表现为 N-MORB 向 E-MORB 过渡的特征。

样品 Zr、Hf 和 Nb 丰度变化范围分别为 $65.4\times10^{-6}$~$143\times10^{-6}$,$1.82\times10^{-6}$~$3.76\times10^{-6}$,$5.11\times10^{-6}$~$10.3\times10^{-6}$,5 件样品的元素丰度值与中等 Zr、Hf 和 Nb 丰度的 E-MORB($73.0\times10^{-6}$,$2.03\times10^{-6}$,$8.30\times10^{-6}$)较相近,其中相容元素 Ni、Cr 和 Co 含量相对较低,Ni = $48.4\times10^{-6}$~$105\times10^{-6}$,Cr 变化范围较大,介于 $7.38\times10^{-6}$~$736\times10^{-6}$,Co =

表 2 湖北十堰黄龙-方滩地区辉长岩主量元素(%)、微量($\times10^{-6}$)和稀土元素($\times10^{-6}$)组成

Table 2 Analyses and ratios of major element(%), rare earth element($\times10^{-6}$) and trace element($\times10^{-6}$) for gabbro samples from the Huanglong-Fangtan area, Shiyan City of Hubei Province

| 样号 | SY112 | SY113 | SY116 | SY117 | SY118 | 样号 | SY112 | SY113 | SY116 | SY117 | SY118 | 样号 | SY112 | SY113 | SY116 | SY117 | SY118 |
|---|---|---|---|---|---|---|---|---|---|---|---|---|---|---|---|---|---|
| $SiO_2$ | 49.99 | 43.71 | 48.4 | 47.8 | 48.98 | Ni | 48.4 | 105 | 67.7 | 67.2 | 71.8 | Eu | 0.99 | 1.31 | 1.62 | 1.3 | 1.8 |
| $TiO_2$ | 1.27 | 2.65 | 1.86 | 1.54 | 1.9 | Rb | 6.29 | 1.27 | 8.84 | 5.9 | 5.67 | Gd | 3.21 | 3.66 | 5.47 | 4.3 | 5.98 |
| $Al_2O_3$ | 15.03 | 15.32 | 14.63 | 13.94 | 14.6 | Sr | 324 | 646 | 185 | 282 | 272 | Tb | 0.53 | 0.58 | 0.86 | 0.68 | 0.91 |
| $Fe_2O_3$ | 2.41 | 3.76 | 2.75 | 3.15 | 3.06 | Ba | 197 | 43.4 | 269 | 272 | 240 | Dy | 3.18 | 3.67 | 5.2 | 4.22 | 5.57 |
| FeO | 6.21 | 11.32 | 9.23 | 9.2 | 8.93 | Pb | 2.32 | 2.68 | 2.57 | 6.51 | 2.15 | Ho | 0.64 | 0.74 | 1.07 | 0.83 | 1.08 |
| MnO | 0.15 | 0.19 | 0.2 | 0.19 | 0.16 | Th | 0.61 | 0.71 | 1.33 | 0.91 | 1.38 | Er | 1.64 | 1.92 | 2.72 | 2.24 | 2.79 |
| MgO | 7.3 | 6.03 | 6.25 | 7.24 | 6.48 | U | 0.12 | 0.15 | 0.26 | 0.19 | 0.28 | Tm | 0.24 | 0.28 | 0.4 | 0.33 | 0.4 |
| CaO | 11.18 | 11.35 | 8.27 | 9.05 | 8.45 | Nb | 5.11 | 6.17 | 10.3 | 7.47 | 10.3 | Yb | 1.55 | 1.82 | 2.64 | 2.16 | 2.59 |
| $Na_2O$ | 3.24 | 2.37 | 4.03 | 3.4 | 3.67 | Ta | 1.29 | 0.93 | 0.79 | 0.65 | 0.76 | Lu | 0.22 | 0.27 | 0.38 | 0.32 | 0.38 |
| $K_2O$ | 0.4 | 0.3 | 0.66 | 0.52 | 0.45 | Zr | 65.4 | 77 | 143 | 96.2 | 142 | TLREE | 43.22 | 48.84 | 82.36 | 61.81 | 91.66 |
| $P_2O_5$ | 0.14 | 0.14 | 0.27 | 0.19 | 0.27 | Hf | 1.82 | 2.15 | 3.69 | 2.62 | 3.76 | THREE | 11.21 | 12.94 | 18.74 | 15.08 | 19.7 |
| 烧失量 | 1.26 | 1.44 | 2.48 | 2.66 | 2.2 | V | 242 | 808 | 286 | 299 | 293 | $\frac{TLREE}{THREE}$ | 3.86 | 3.77 | 4.39 | 4.1 | 4.65 |
| 总量 | 97.32 | 97.14 | 96.55 | 96.22 | 96.95 | Y | 16.7 | 19.4 | 28.8 | 22.7 | 28.8 | $La_N/Yb_N$ | 3.57 | 3.47 | 4.24 | 3.89 | 4.85 |
| $Mg^{\#}$ | 60.83 | 42.23 | 48.77 | 51.75 | 49.72 | Cr | 736 | 7.38 | 124 | 192 | 115 | $La_N/Sm_N$ | 1.71 | 1.8 | 2.04 | 1.96 | 2.11 |
| Co | 40.5 | 60.4 | 49 | 51.6 | 51.1 | La | 7.72 | 8.8 | 15.6 | 11.7 | 17.5 | $Gd_N/Lu_N$ | 1.8 | 1.68 | 1.78 | 1.66 | 1.95 |

注:① $Mg^{\#}=100\times Mg/(Mg+Fe^{2+})$; ② Standardization of REE values after Sun and McDonough(1989); ③ $\delta Ce=Ce_N/SQRT(La_N\times Pr_N)$; $\delta Eu=Eu_N/SQRT(Sm_N\times Gd_N)$; (4) $Fe_2O_3{}^T=Fe_2O_3+1.1002\times FeO$。

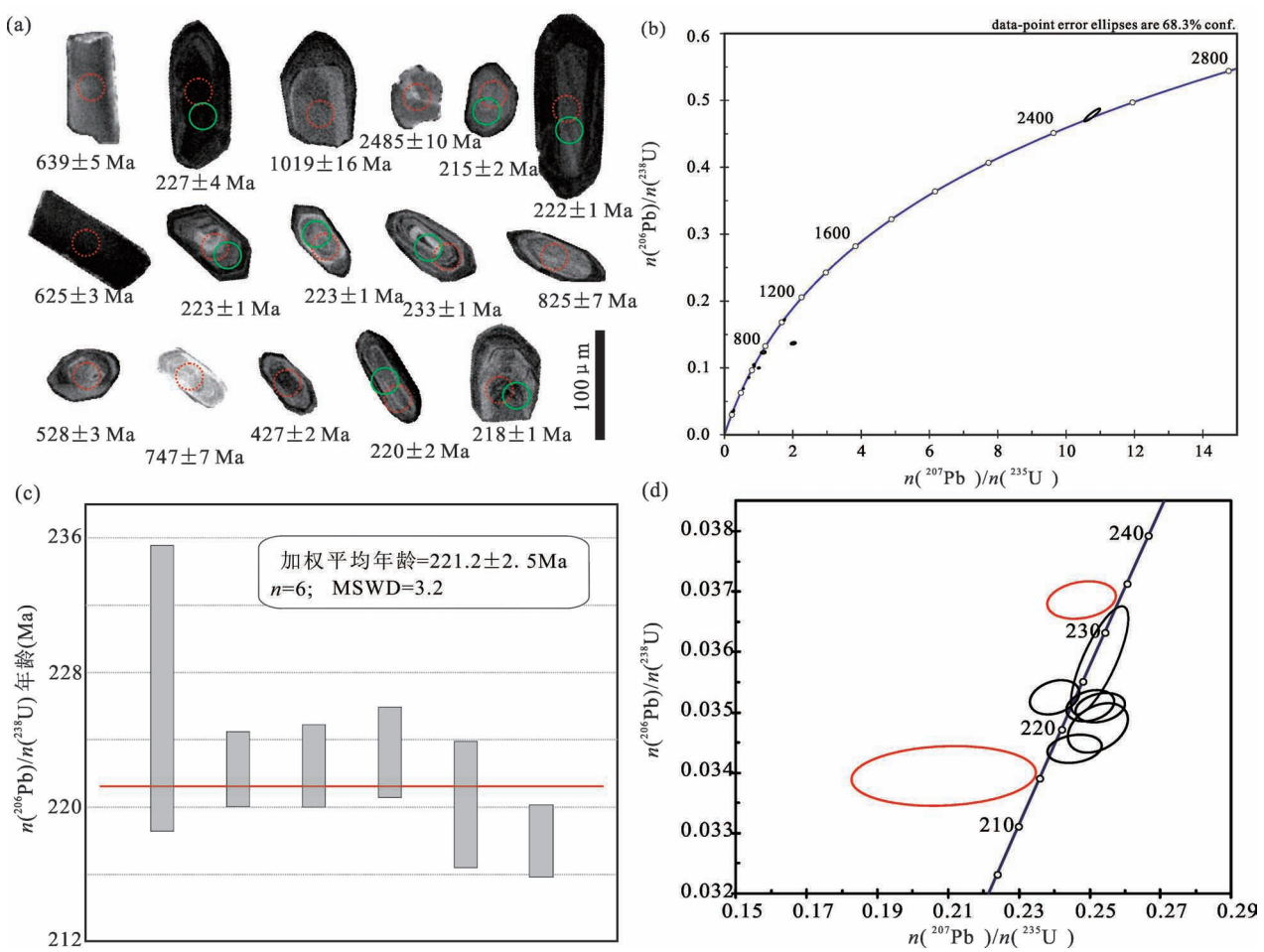


图 4 十堰黄龙—方滩地区辉长岩锆石 U-Pb 年龄及 CL 图像(红色圆圈为锆石测年点,绿色圆圈为 Hf 同位素测试点)

Fig. 4 U-Pb age and CL images of zricon from gabbro in Huanglong-Fangtan area, Shiyan(red circles represent zircon dating spots, and the green one represent Hf isotope testing spot in fig 4a)

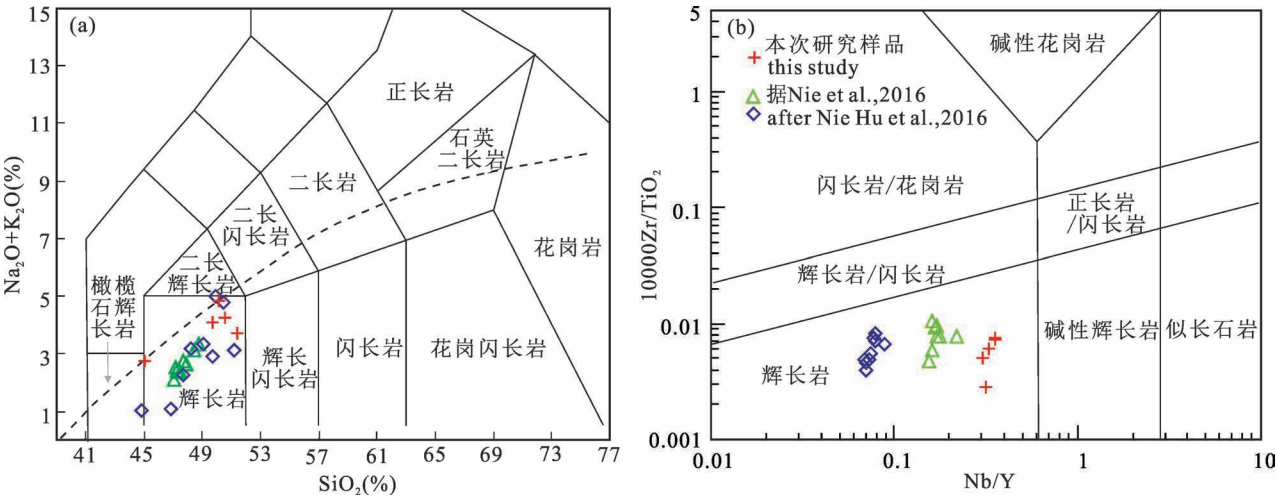


图 5 十堰黄龙-方滩地区辉长岩 TAS 图解(a,底图据 Middlemost, 1994)和 10000Zr/$TiO_2$- Nb/Y 图解(b,底图据 Pearce at al., 1996)

Fig. 5 Classification diagrams of TAS and 10000Zr/$TiO_2$ versus Nb/Y for gabbro in Huanglong-Fangtan area. Shiyan City (a, after Middlemost, 1994; b, after Pearce at al., 1996)

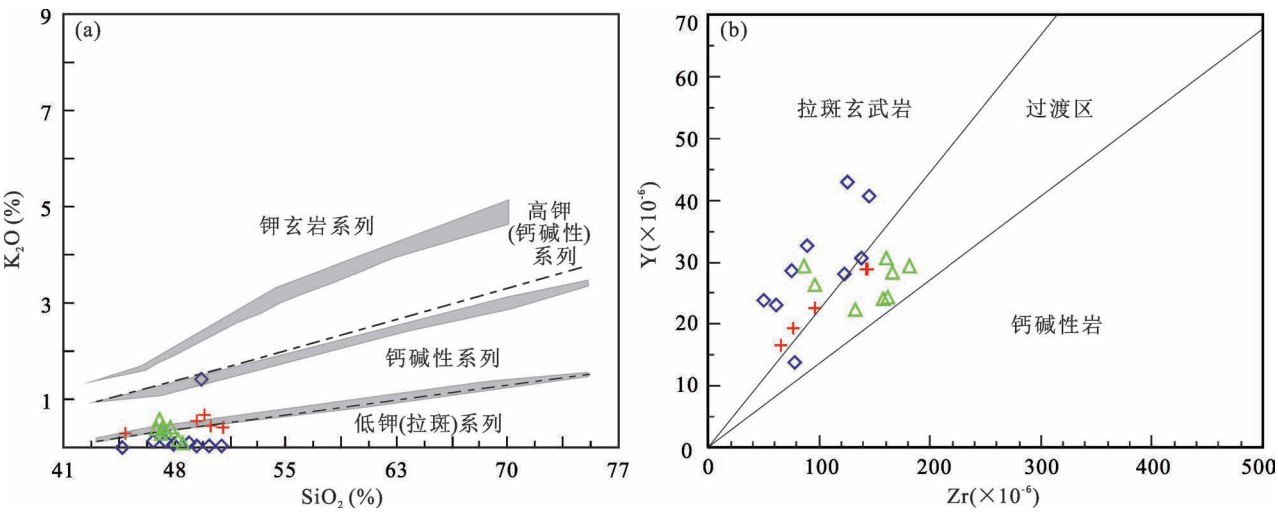


图 6 十堰黄龙-方滩地区辉长岩 $K_2O$-$SiO_2$ 图解(a,底图据 Rickwood, 1989)和 Y-Zr 图解(b,底图据 Barrett, 1999;图例同图 5)

Fig. 6 Magma series diagrams of $K_2O$ versus $SiO_2$ and Y versus Zr for gabbro in Huanglong-Fangtan area, Shiyan City (a, after Rickwood, 1989; b, after Barrett, 1999; Legends are the same to those in Fig. 5)

$40.5\times10^{-6}$~$60.4\times10^{-6}$。样品原始地幔标准化微量元素配分曲线整体与 E-MORB 配分曲线相似,呈平坦微右倾型分配模式(图 7b)。其中 Rb、Sr 等大离子亲石元素表现为亏损,而 Pb 元素富集成峰。

### 3.3 锆石 Hf 同位素组成

锆石 Hf 同位素测试分析点位和 U-Pb 点相对应,测试结果见表 3。代表辉长岩岩浆结晶年龄的锆石 $n(^{176}Yb)/n(^{177}Hf)$ 值范围为 0.097167~0.241165, $n(^{176}Lu)/n(^{177}Hf)$ 值变化范围为 0.001523~0.004431, $n(^{176}Hf)/n(^{177}Hf)$ 值范围为 0.282354~0.282479。根据锆石结晶年龄计算,获得 $\varepsilon_{Hf}(t)$ 值在-10.27 至-6.18,峰值为-9.29;锆石 Hf 模式年龄 $T_{DM1}$ = 1202~1332 Ma, $T_{DM2}$ = 1640~1895 Ma(图 8), $f_{Lu/Hf}$ = -0.95~-0.87,明显小于下地壳值(-0.34)和上地壳值(-0.72),其两阶段模式年龄更能反映源区物质从亏损地幔被抽取的时间或源区物质在地壳的平均存留年龄(Amelin et al., 1999)。

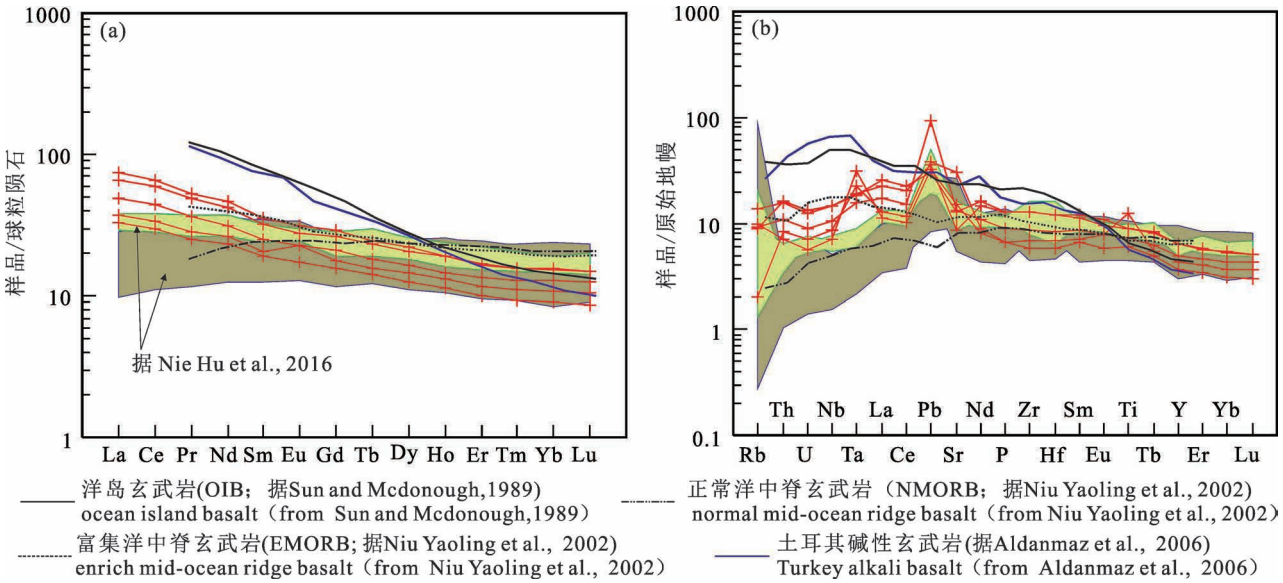


图 7 十堰黄龙-方滩地区辉长岩稀土配分曲线(a)和微量元素蛛网图(b)

Fig. 7 Chondrite-normalized rare earth element patterns(a) and primitive mantle-normalized spidergrams (b) for gabbro in Huanglong-Fangtan area, Shiyan City

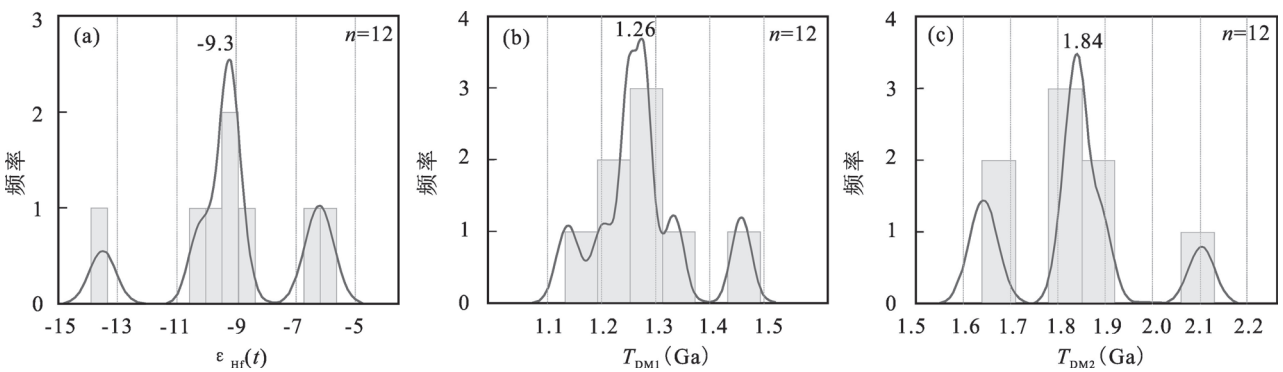


图 8 十堰黄龙-方滩地区辉长岩锆石 Hf 和模式年龄组成

Fig. 8 Zricon Hf and model age for gabbro from the Huanglong-Fangtan area, Shiyan City

(a) 锆石 Hf 组成；(b) 锆石 Hf 单阶段模式年龄组成；(c) 锆石 Hf 两阶段模式年龄组成

(a) Zircon Hf isotope composition; (b) Zircon Hf single-stage model age composition; (c) Zircon Hf two-stage model age composition

# 4 岩石成因

## 4.1 岩浆演化

分析结果显示，辉长岩样品 Eu 具有弱负异常，$Mg^{\#}=42\sim61$，$Ni=48.4\times10^{-6}\sim105\times10^{-6}$，二者均低于原始岩浆值（$Mg^{\#}$值>65，Ni 含量>$235\times10^{-6}$；Hess，1992；邓晋福等，2004），说明母岩浆在岩浆房内或上升至地表的过程中曾发生明显的分离结晶作用。在 La/Sm-La 图解上(图 9a)辉长岩样品表现出部分熔融的特点，指示初始岩浆先后经历了部分熔融作用和分离结晶作用(邓晋福等，2015)。基性岩中，大离子亲石元素如 Rb、Ba、Sr 等更容易受到后期蚀变与变质作用改造，而 V、Cr 等过渡元素和 Zr、Hf、Nb、Ta、Ti 等高场强元素以及稀土元素的活动性不会改变，常用来分析岩浆演化过程(Pearce and Cann，1973；Riley et al.，2001)。样品集中投影在 Nb/U-Nb 图解中的 MORB 区域附近(图 9b)，$(La/Sm)_N<4.5$，且 Nb、Ta 也并未出现亏损，反而 Ta 相对富集，这都表明岩浆演化过程中同化混染作用是有限的(Keppler，1996)。因此本文测试样品先后经历了源岩部分熔融和母岩浆分离结晶作用，岩浆上升过程中未受到地壳物质明显的同化混染作用。

## 4.2 岩浆源区

辉长岩样品的岩石稀土元素 ∑LREE/∑HREE 和$(La/Yb)_N$显示轻稀土富集重稀土亏损的特征，具有类似于 E-MORB 稀土配分曲线。在$(Tb/Yb)_N$

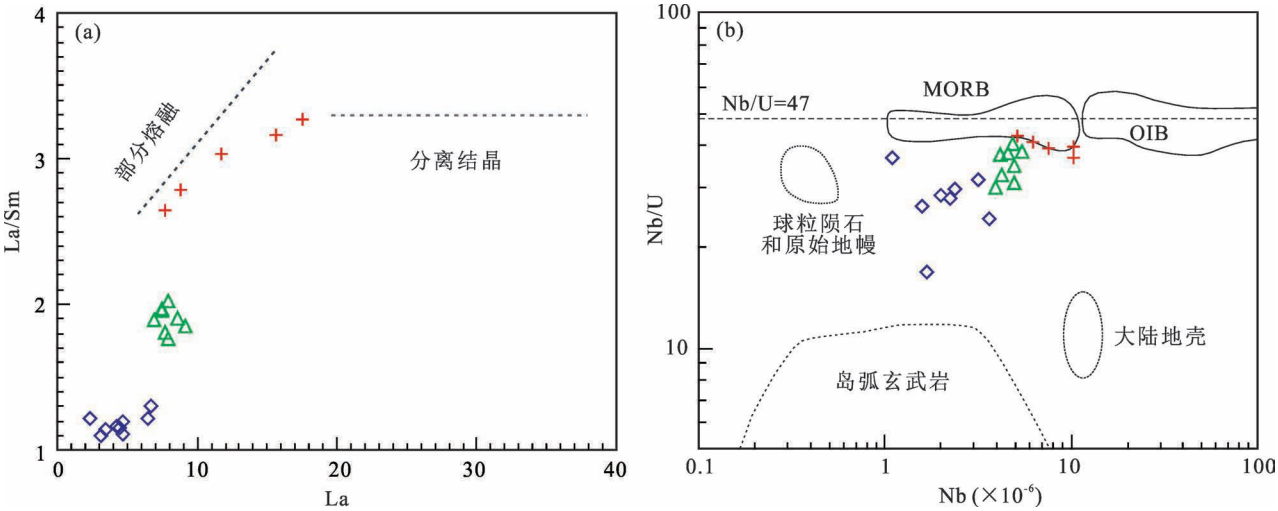


图 9 十堰黄龙-方滩地区辉长岩 La/Sm-La 图解(a,据 Geng Hongyan et al. , 2009)和 Nb/U-Nb 图解(b,据 Hofmann et al. , 1986; 图例同图 5)

Fig. 9 The binary diagram of La/Sm-La and Nb/U-Nb for gabbro from the Huanglong-Fangtan area, Shiyan City (a,after Geng Hongyan et al. , 2009; b,after Hofmann et al. , 1986; Legends are the same to those in Fig. 5)

**表 3 湖北十堰黄龙-方滩地区辉长岩锆石 Lu-Hf 同位素组成**

**Table 3 Lu-Hf isotope compositions of the zircons for gabbro sample from the Huanglong-Fangtan area zircon, Shiyan City of Hubei province**

| 测点号 | 年龄 (Ma) | $n(^{176}Yb)/n(^{177}Hf)$ | $n(^{176}Lu)/n(^{177}Hf)$ | | $n(^{176}Hf)/n(^{177}Hf)$ | | $\varepsilon_{Hf}(0)$ | $\varepsilon_{Hf}(t)$ | $T_{DM1}$ (Ma) | $T_{DM2}$ (Ma) | $f_{Lu/Hf}$ |
|---|---|---|---|---|---|---|---|---|---|---|---|
| | | 测值 | 测值 | 2σ | 测值 | 2σ | | | | | |
| SY112-02 | 227 | 0.221985 | 0.003721 | 0.000057 | 0.282377 | 0.000024 | -14 | -9.6 | 1332 | 1858 | -0.89 |
| SY112-05 | 215 | 0.097167 | 0.001523 | 0.000011 | 0.282354 | 0.000021 | -14.8 | -10.3 | 1286 | 1895 | -0.95 |
| SY112-06 | 222 | 0.112371 | 0.001861 | 0.000018 | 0.282389 | 0.000021 | -13.5 | -8.9 | 1247 | 1816 | -0.94 |
| SY112-08 | 223 | 0.08694 | 0.001791 | 0.00004 | 0.282465 | 0.000029 | -10.9 | -6.2 | 1137 | 1646 | -0.95 |
| SY112-09 | 223 | 0.136304 | 0.002592 | 0.000035 | 0.282263 | 0.000025 | -18 | -13.5 | 1457 | 2103 | -0.92 |
| SY112-10 | 233 | 0.122569 | 0.002046 | 0.000016 | 0.282375 | 0.000016 | -14.1 | -9.3 | 1274 | 1844 | -0.94 |
| SY112-11 | 825 | 0.145519 | 0.002639 | 0.000072 | 0.281679 | 0.000033 | -38.7 | -21.9 | 2302 | 3073 | -0.92 |
| SY112-12 | 528 | 0.084657 | 0.001667 | 0.000138 | 0.281995 | 0.000021 | -27.5 | -16.5 | 1800 | 2516 | -0.95 |
| SY112-13 | 747 | 0.091259 | 0.001342 | 0.000052 | 0.282104 | 0.00002 | -23.6 | -7.8 | 1632 | 2142 | -0.96 |
| SY112-14 | 427 | 0.171943 | 0.003307 | 0.00005 | 0.282023 | 0.00003 | -26.5 | -18.1 | 1841 | 2539 | -0.9 |
| SY112-15 | 220 | 0.241165 | 0.004431 | 0.000054 | 0.282479 | 0.000026 | -10.4 | -6.2 | 1202 | 1640 | -0.87 |
| SY112-16 | 218 | 0.103227 | 0.001641 | 0.000015 | 0.282382 | 0.000019 | -13.8 | -9.3 | 1251 | 1833 | -0.95 |

注:计算公式如下(黄道袤等,2016;杨佳林等,2018):

$$\varepsilon_{Hf}(t) = 10000 \cdot \left\{ \frac{\left[\frac{n(^{176}Hf)}{n(^{177}Hf)}\right]_S - \left[\frac{n(^{176}Lu)}{n(^{177}Hf)}\right]_S \cdot (e^{\lambda t} - 1)}{\left[\frac{n(^{176}Hf)}{n(^{177}Hf)}\right]_{CHUR,0} - \left[\frac{n(^{176}Lu)}{n(^{177}Hf)}\right]_{CHUR} \cdot (e^{\lambda t} - 1)} - 1 \right\};\quad T_{DM1} = \frac{1}{\lambda} \cdot \ln\left\{1 + \frac{\left[\frac{n(^{176}Hf)}{n(^{177}Hf)}\right]_S - \left[\frac{n(^{176}Hf)}{n(^{177}Hf)}\right]_{DM}}{\left[\frac{n(^{176}Lu)}{n(^{177}Hf)}\right]_S - \left[\frac{n(^{176}Lu)}{n(^{177}Hf)}\right]_{DM}}\right\};$$

$$T_{DM\,2CC} = T_{DM1} - (T_{DM1} - t) \cdot \frac{f_{CC} - f_S}{f_{CC} - f_{DM}};\quad f_{Lu/Hf} = \left[\frac{n(^{176}Lu)}{n(^{177}Hf)}\right]_S \Big/ \left[\frac{n(^{176}Lu)}{n(^{177}Hf)}\right]_{CHUR} - 1。$$

其中:$\lambda(^{176}Lu) = 1.867\times10^{-11}$/ a (Söderlund et al. ,2004); $\left[\frac{n(^{176}Lu)}{n(^{177}Hf)}\right]_S$ 和 $\left[\frac{n(^{176}Hf)}{n(^{177}Hf)}\right]_S$ 为样品测量值; $\left[\frac{n(^{176}Lu)}{n(^{177}Hf)}\right]_{CHUR} = 0.0332$, $\left[\frac{n(^{176}Hf)}{n(^{177}Hf)}\right]_{CHUR,0} = 0.282772$(Blichert-Toft et al. ,1997); $\left[\frac{n(^{176}Lu)}{n(^{177}Hf)}\right]_{DM} = 0.0384$, $\left[\frac{n(^{176}Hf)}{n(^{177}Hf)}\right]_{DM} = 0.28325$(Griffin et al. , 2000); $\left[\frac{n(^{176}Lu)}{n(^{177}Hf)}\right]_{平均地壳} = 0.015$; $f_{CC} = \frac{\left[\frac{n(^{176}Lu)}{n(^{177}Hf)}\right]_{平均地壳}}{\left[\frac{n(^{176}Lu)}{n(^{177}Hf)}\right]_{CHUR}} - 1$; $f_S = f_{Lu/Hf}$; $f_{DM} = \frac{\left[\frac{n(^{176}Lu)}{n(^{177}Hf)}\right]_{DM}}{\left[\frac{n(^{176}Lu)}{n(^{177}Hf)}\right]_{CHUR}} - 1$; $t$ 为锆石结晶年龄。

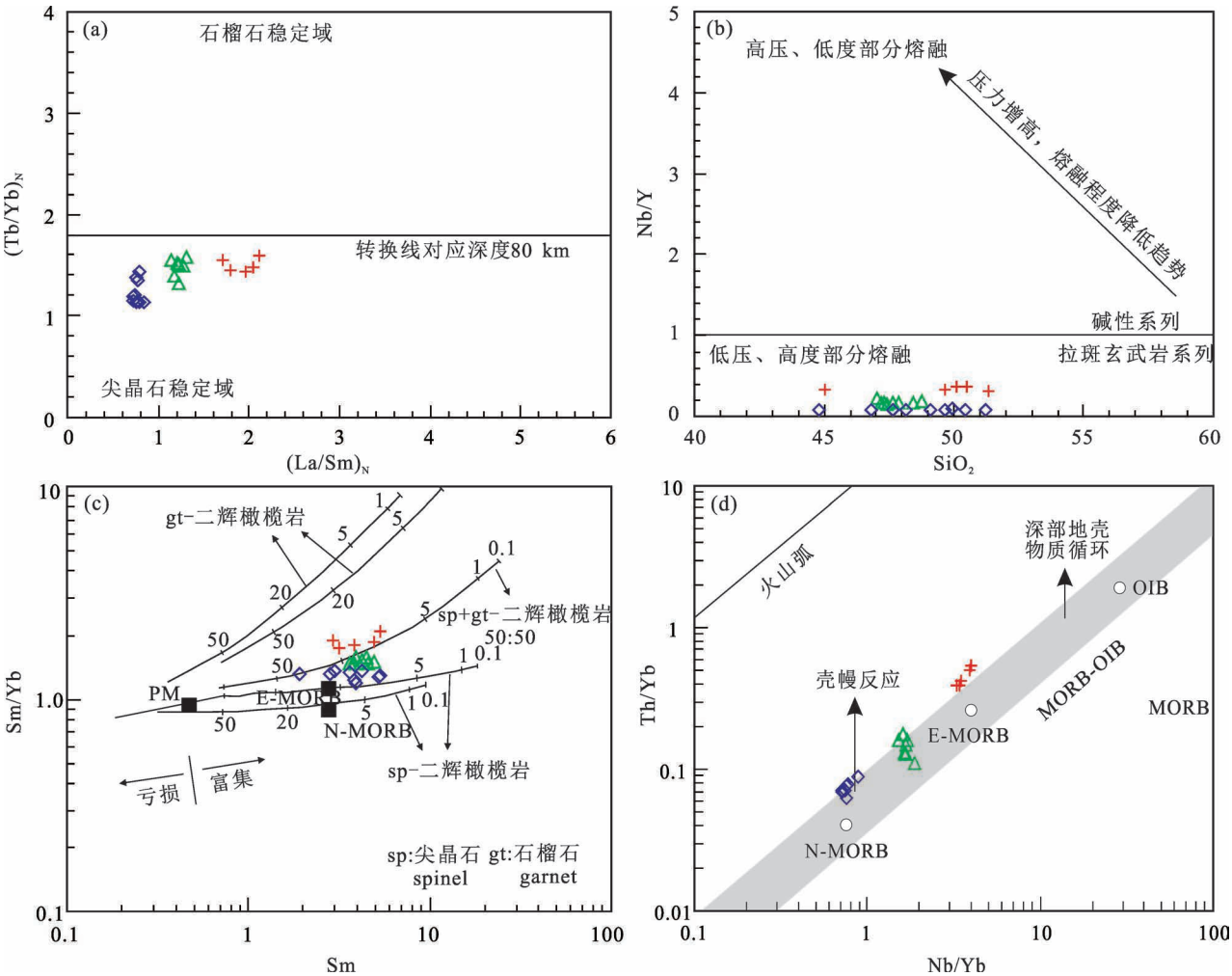


图 10 十堰黄龙-方滩地区辉长岩源区$(Tb/Yb)_N$-$(La/Sm)_N$, $SiO_2$-Nb/Y, Sm/Yb-Sm 和 Th/Yb - Nb/Yb 判别图解(a,据 Furman et al., 2004; b,据 Greenough et al., 2005; c,据 Aldanmaz et al., 2000; d,据 Pearce, 2008 修改;图例同图 5)

Fig. 10 The binary diagrams of$(Tb/Yb)_N$ versus$(La/Sm)_N$, $SiO_2$-Nb/Y, Sm/Yb versus Sm and Dy/Yb versus La/Yb for gabbro from the Huanglong-Fangtan area, Shiyan City(a,after Furman et al., 2004; b,after Greenough et al., 2005; c,after Aldanmaz et al., 2000; d,after Pearce, 2008; Legends are the same to those in Fig. 5)

-$(La/Sm)_N$ 图解上(图 10a),样品投影在尖晶石稳定域内表明其岩浆熔融深度小于 80 km。在 $SiO_2$-Nb/Y 图解上(图 10b),样品均投影在低压、高度部分熔融的拉斑玄武岩浆区域,指示岩浆可能经过较高程度部分熔融形成。Sm/Yb-Sm 图解显示样品源区具有尖晶石二辉橄榄岩和石榴子石二辉橄榄岩混合特征,岩浆为二者发生 20%~30%的部分熔融形成(图 10c),结合图 10b,笔者等认为该岩浆为尖晶石二辉橄榄岩低压、中等程度部分熔融形成。在 Th/Yb-Nb/Yb 图解上(图 10d),样品主要分布在 E-MORB 序列附近,表明岩浆源区来自于亏损地幔部分熔融,并受富集地幔组分影响(Pearce et al., 1984;Choe et al., 2007)。Nie Hu 等(2016)报道的武当山南部发育的中生代镁铁质岩与本文测试样品具有相似特征,但其岩浆源区来源于以尖晶石二辉橄榄岩部分熔融为主,且主要来源于亏损地幔端元,富集地幔组分影响较少。总体来讲,三组样品体现出自南向北,受富集地幔组分影响越来越大趋势特征。

锆石的 Hf 同位素组成很少受到后期地质作用影响,是探讨岩浆源区属性的重要证据。本文样品锆石同位素 $\varepsilon_{Hf}(0)$ 和 $\varepsilon_{Hf}(t)$<0,暗示源区可能是古老地壳或有古老地壳物质加入,或者源区来源于富集岩石圈地幔;样品两阶段模式年龄更能反映源区物质从亏损地幔被抽取的时间或源区物质在地壳的平均存留年龄,而岩体结晶年龄的锆石 Hf 两阶段模

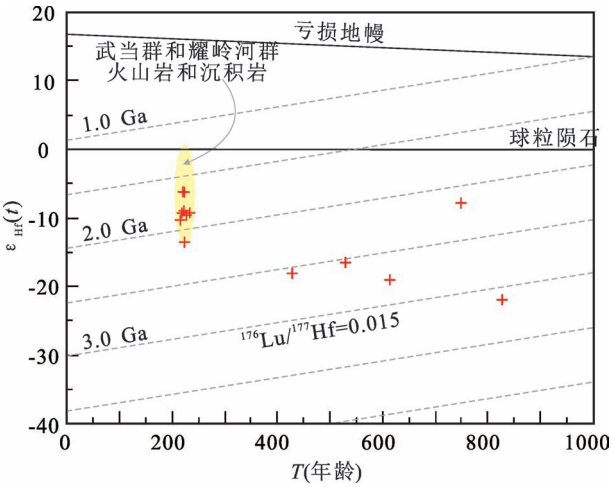


图 11 十堰黄龙-方滩地区辉长岩锆石 $\varepsilon_{Hf}(t)$ 与年龄关系图

Fig. 11 Plot of $\varepsilon_{Hf}(t)$ and U-Pb age of zircon for gabbro from the Huanglong-Fangtan area, Shiyan City

武当群和耀岭河群火山岩和沉积岩 $\varepsilon_{Hf}(t)$ 组成区域据 Wang Lijuan et al., 2013 数据换算($t$=220 Ma)

Date $\varepsilon_{Hf}(t)$ of The Wudang Group and The Yaolinghe Group from Wang Lijuan et al, 2013&. ($t$=220 Ma)

式年龄(2103~1640 Ma)远大于锆石结晶年龄(220 Ma),表明岩浆受到地壳混染或来源于富集地幔(吴福元等,2007)。锆石的 Hf 同位素值与前人报道的十堰-丹江口地区新元古代武当群和耀岭河群火山岩锆石 Hf 同位素组成具有相似性(图 11),且与其两阶段模式年龄一致(Wang Lijuan et al., 2013),指示本文辉长岩可能与新元古代火山岩来自同一岩浆源区。而区域上武当群和耀岭河群火山岩 Nd-Hf 同位素反映二者岩石成因可能存在差异,大部分以幔源物质占主导,小部分来自地壳物质重熔成因(祝禧艳等,2009;Wang Lijuan et al., 2013)。因此本文辉长岩样品岩浆源区也可能以幔源物质成分为主,而非地壳混染,这与前文全岩地球化学数据特征相吻合。综上,该套辉长岩的可能来源于源区发生了改造的幔源岩浆,为亏损地幔与富集地幔组分混合的源区性质。

## 5　讨论

秦岭造山带经历了新元古代-中生代的俯冲-增生造山、碰撞造山以及陆内造山等多个构造演化阶段(张国伟等,2001;Ratschbacher et al., 2003; 王宗起等,2009;杨经绥等,2010;Bader et al., 2013; Dong Yunpeng et al., 2015; 张国伟等,2019)。以商丹断裂为界,将秦岭划分为南秦岭和北秦岭(李春昱等,1978;许志琴等,1988;张国伟,1991),勉略断裂带则将扬子板块与南秦岭分隔(李春昱等,1978)。王宗起等(2009)将增生造山的理论应用于秦岭造山带,认为勉略带及附近相关构造-岩石单元为一条增生杂岩带(王涛等,2011;Yan Zhen et al., 2012;许志琴等,2015)。不同构造演化观点的争议在于南秦岭勉略洋盆的性质和形成时限(Wang Gang et al., 2017;王刚等,2019),然而大量同碰撞和后碰撞花岗岩的发育(Qin Jiangfeng et al., 2013)和变火山岩记录的变质时代(李曙光等,1996)等证据表明勉略洋已于晚三叠世闭合并导致华北板块与扬子板块全面碰撞,这一观点在地学界已达成共识(张国伟等,1995;王宗起等,2009;Dong Yunpeng et al., 2011;Li Sanzhong et al., 2018)。

本次研究的辉长岩样品岩石地球化学、稀土配分曲线和微量元素蛛网图显示样品具有 E-MORB 特征,样品在 Nb/U-Nb, Sm/Yb-Sm 和 Th/Yb-Nb/Yb 图中均投影在 MORB 附近;在 Hf/3-Th-Nb/16 判别图解中大部分落入 E-MORB 区域内(图 12a);在 Agrawal 等(2008)基于已知基性和超基性玄武岩的不活跃微量元素创建的判别图解中,亦落在 MORB 区域(图 12b)。结合空间展布,与 Nie Hu 等(2016)报道的镁铁质岩共同代表了 N-MORB 向 E-MORB 过渡的线性演化特征。

前人研究表明,E-MORB 型岩浆主要发育于大洋中脊及附近的海山(Niu Yaoling et al., 1999; Hemond et al., 2006)、现代大洋弧后盆地也有少量发育,如 Mariana 和 Lau Basin(Gribble et al., 1996; Hawkins, 2003),此外汇聚大陆边缘如环太平洋造山带也出现具有 E-MORB 特征的岩石,主要受洋脊(扩张脊)俯冲影响(Cole et al., 2006),但这些岩石只是具有 E-MORB 特征,并非真正大洋性质岩石。前文述及,印支期勉略洋盆开始关闭,经过俯冲-增生造山过程至晚三叠世闭合,结合本文岩石成因探讨,该套 E-MORB 型辉长岩样品以及 Nie Hu 等(2016)报道的武当山南部发育的中生代 N-MORB 镁铁质岩并非产生于大洋脊环境,亦不符合弧后扩张的构造背景。Nie Hu 等(2016)将武当山南部发育的中生代镁铁质岩解释为勉略洋闭合后由碰撞挤压转换为伸展的构造环境,这与传统观点认为武当山为前寒武纪基底,经历了印支期陆内构造作用的认识较一致。然而,有学者认为武当山整体或局部是混杂带。如周鼎武等(1998)认为武当群由不同

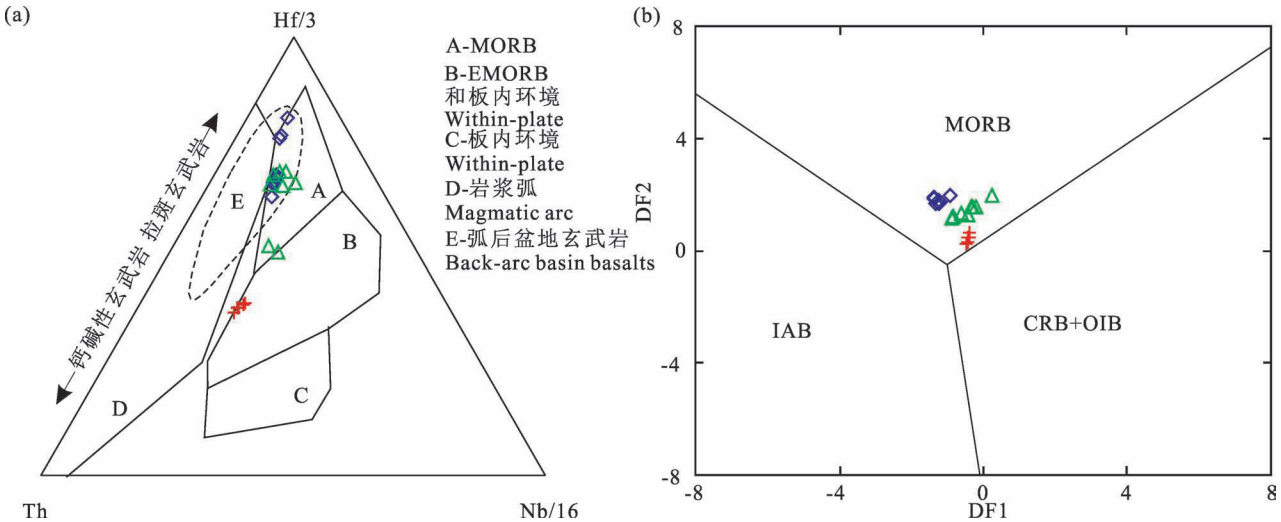


图 12 十堰黄龙-方滩地区辉长岩 Hf/3-Th-Nb/16 和 *DF*1-*DF*2 构造判别图解(a,据 Metzger et al., 2002; b,据 Agrawal et al., 2008 修改;图例同图 5)

Fig. 12 Plots of Hf/3-Th-Nb/16 and *DF*1-*DF*2 for gabbro from the Huanglong-Fangtan area, Shiyan City (a, after Metzger et al., 2002; b, after Agrawal et al., 2008; Legends are the same to those in Fig. 5)

MORB-洋中脊玄武岩;IAB-岛弧玄武岩;OIB-洋岛玄武岩;CRB-大陆裂谷玄武岩

MORB-mid-ocean ridge basalt; IAB-island arc basalt; OIB-ocean island basalt; CRB-continental rift basalt; $DF1 = 0.3518\ln(La/Th) + 0.6013\ln(Sm/Th) - 1.3450\ln(Yb/Th) + 2.1056\ln(Nb/Th) - 5.4763$; $DF2 = -0.3050\ln(La/Th) - 1.1801\ln(Sm/Th) + 1.6189\ln(Yb/Th) + 1.2260\ln(Nb/Th) - 0.9944$

时代、不同古构造环境的地质体以构造关系组合在一起、时间跨度大的复杂构造组合体;或认为两郧-随枣或丹江口-随州一带(王荃等,2010)存在俯冲带和增生混杂带。近年来,黄龙-方滩地区先后报道了中晚泥盆世海相沉积组合与火山物质岩片(王刚等,2018)和中二叠世火山作用产物(王刚等,2019)以及大量新元古代不同岩性及成因的块体(~640 Ma 的 OIB 型辉绿岩块,沉积时代晚于~612 Ma 的含石英大理岩块)和碎屑锆石时代(最年轻峰值 220 Ma;王宗起等❹),表明该地区存在中生代构造混杂岩带,王东升等(2019)结合前人大量中生代变质和变形年代学证据及变质温压条件认为,黄龙地区岩石为中低级变质且表现出不均衡特征,是受控于该地区晚古生代-中生代俯冲增生过程。基于上述研究成果,晚古生代-中生代武当山可能并非统一结晶基底,武当南缘以及十堰-两郧断裂之间构造混杂岩带的识别(王宗起等❹;湖北省地质调查院❺;王刚等,2018,2019;许光等,2018;王东升等,2019),表明武当山内部或整体在晚古生代-中生代可能经历了勉略洋盆关闭导致的俯冲-碰撞造山作用,因此本文样品形成的构造环境类似于环太平洋造山带等汇聚大陆边缘,并形成了具有 E-MORB 特征的岩石,且受到勉略洋壳俯冲的影响,为俯冲-碰撞造山阶段产物。

## 6 结论

(1)十堰黄龙-方滩构造混杂带内侵入发育的辉长岩的 SHRIMP 锆石 U-Pb 年龄为 221.2±2.5 Ma,表明其形成于晚三叠世。

(2)该套辉长岩具有轻稀土元素富集重稀土亏损特征,Zr、Hf、Nb 等高场强元素丰度为中高等,Rb、Sr 等大离子亲石元素表现为亏损,结晶年龄锆 $\varepsilon_{Hf}(t)$ 值相对均一在-13.5 至-6.18 之间,指示岩浆为尖晶石二辉橄榄岩低压、中等程度部分熔融形成,来源于亏损地幔和富集组分混合的地幔源区。

(3)研究区中生代镁铁质岩 MORB 性质的岩石形成的构造环境可能类似于汇聚边缘环境,且受到勉略洋壳俯冲的影响,为俯冲-碰撞造山阶段产物。

**致谢**:在成文过程中,杨经绥院士、陈雷研究员、冯光英副研究员和刘飞博士提出了许多建设性意见和建议并给予笔者等悉心的帮助,在此表示衷心的感谢!

### 注 释 / Notes

❶湖北省地质矿产局区域地质矿产调查所. 1985. 竹山幅 1∶20 万

区域地质调查报告. 武汉:湖北地矿局区域地质矿产调查所.

❷ 湖北省地质矿产局区域地质矿产调查所. 1990. 黄龙滩幅 1∶5 万区域地质调查报告. 武汉:湖北地矿局区域地质矿产调查所.

❸ 湖北省地质调查院. 2009. 十堰市幅 1∶25 万区域地质调查报告. 武汉: 湖北省地质调查院.

❹ 王宗起, 武昱东, 王刚, 张晗, 王涛, 王东升, 贾少华, 张玉涛. 2016. 武当-桐柏-大别关键地区区域地质调查成果报告. 北京: 中国地质科学院矿产资源研究所.

❺ 湖北省地质调查院. 2016. 水坪幅、竹山县幅、蔡家坝幅、峪口幅 1∶5 万区域地质矿产调查报告. 武汉:湖北省地质调查院.

## 参 考 文 献 / References


(The literature whose publishing year followed by a "&" is in Chinese with English abstract; The literature whose publishing year followed by a "#" is in Chinese without English abstract)

蔡志勇, 罗洪, 熊小林, 吴德宽, 吴贤亮, 孙三才, 杨军. 2006. 武当山群上部变沉积岩组时代归属问题单锆石 U-Pb 年龄的制约. 地层学杂志, 30(1):60~63.

陈晋镳, 秦正永, 王寿琼. 1991. 武当群地质特征. 天津:天津科技出版社: 1~130.

邓晋福, 罗照华, 苏尚国. 2004. 岩石成因、构造环境与成矿作用. 北京: 地质出版社: 1~381.

邓晋福, 刘翠, 冯艳芳, 肖庆辉, 狄永军, 苏尚国, 赵国春, 段培新, 戴蒙. 2015. 关于火成岩常用图解的正确使用: 讨论与建议. 地质论评, 61(4): 717~734.

付建明, 张业明, 蔡锦辉, 陈盛峰. 1999. 武当地区武当岩群变火山岩原岩性质及其构造环境研究. 地质论评, 45(7): 668~673.

侯可军, 李延河, 田有荣. 2009. LA-MC-ICP-MS 锆石微区原位 U-Pb 定年技术. 矿床地质, 28(4): 481~492.

黄道袤, 万渝生, 张德会, 董春艳, 赵元艺. 2016. 华北克拉通南缘下汤地区古元古代构造热事件-地球化学特征、锆石 SHRIMPU-Pb 定年和 Hf 同位素研究. 地质论评, 62(6): 1439~1461.

胡健民, 孟庆任, 马国良, 张森琦, 高殿松. 2002. 武当地块基性岩席群及其地质意义. 地质论评, 48(4): 353~360.

胡健民, 郭力宇, 宋子新, 李侠, 刘护军. 1995. 扬子地块北缘武当山岩群与耀岭河岩群不整合接触关系的地质意义. 西安地质学院学报, 17(1): 22~27.

胡健民, 赵国春, 孟庆任, 罗洪, 王宗合. 2003. 武当地块基性侵入岩群的地址特征与构造意义. 岩石学报, 19(4): 601~611.

胡健民, 赵国春, 马国良, 张森琦, 高殿松. 2004. 秦岭造山带武当地区古生代伸展构造. 地质科学, 39(3): 305~319.

李春昱, 刘仰文, 朱宝清. 1978. 秦岭及祁连山构造发展史. 见: 国际交流地质学术论文集(1): 区域构造、地质力学. 北京: 地质出版社: 174~187.

李曙光, 孙卫东, 张国伟, 陈家义, 杨永成. 1996. 南秦岭勉略构造带黑沟峡变质火山岩的年代学和地球化学-古生代洋盆及其闭合时代的证据. 中国科学(D 辑), 26(3): 223~230.

凌文黎, 任邦方, 段瑞春, 柳小明, 毛新武, 彭练红, 刘早学, 程建萍, 杨红梅. 2007. 南秦岭武当山群、耀岭河群及其基性侵入岩群锆石 U-Pb 同位素年代学及其地质意义. 科学通报, 52(17): 1445~1456.

刘嘉威, 张宏福. 2018. 南秦岭新元古代基性侵入岩的岩石成因及其构造背景: 锆石 U-Pb 年代学和 Hf-O 同位素地球化学制约. 西北大学学报(自然科学版), 48(2): 268~283.

宋彪, 张玉海, 万渝生. 2002. 锆石 SHRIMP 样品靶制作年龄测定及有关现象讨论. 地质论评, 48(增刊): 26~30.

苏文, 刘景波, 陈能松, 郭顺, 巴金, 张璐, 刘新, 施雨新. 2013. 东秦岭-大别山及其两侧的岩浆和变质事件年代学及其形成的大地构造背景. 岩石学报, 29(5): 1573~1593.

王存智, 杨坤光, 徐扬, 程万强. 2009. 北大巴基性岩墙群地球化学特征、LA-ICP-MS 锆石 U-Pb 定年及其大地构造意义. 地质科技情报, 28(3): 19~26.

王东升, 王宗起, 王刚, 武昱东, 杨皓. 2019. 南秦岭构造带十堰-武当地区岩石变质作用. 地球科学与环境学报, 41(9): 379~395.

王刚, 王宗起, 武昱东, 王东升, 王涛, 王嘉玮, 张航. 2018. 武当山腹地晚古生代沉积与火山物质的识别:微体化石和锆石年代学证据. 地质学报, 92(6): 1163~1175.

王刚, 张晗, 王宗起, 武昱东, 王东升, 王嘉玮. 2019. 武当山十堰地区二叠纪 E-MORB 型玄武岩识别及构造意义. 地质论评, 65(1): 65~84.

王坤明, 王宗起, 张英利, 王刚. 2014. 北大巴山高桥地区镁铁质岩单斜辉石矿物化学特征及其指示意义. 岩石矿物学杂志, 33(3): 527~539.

王荃, 刘雪亚. 2010. 是岩浆侵入还是构造侵位? 地质论评, 56(3): 329~338.

王涛, 王宗起, 闫全人, 闫臻, 覃小锋, 张英利, 向忠金. 2011. 南秦岭白水江群变基性火山岩块体的形成时代及其地球化学特征. 岩石学报, 27(3): 645~656.

王宗起, 闫全人, 闫臻, 王涛, 姜春发, 高联达, 李秋根, 陈隽璐, 张英利, 刘平, 谢春林, 向忠金. 2009. 秦岭造山带主要大地构造单元的新划分. 地质学报, 83(11): 1527~1546.

吴福元, 李献华, 郑永飞, 高山. 2007. Lu-Hf 同位素体系及其岩石学应用. 岩石学报, 23(2): 185~220.

许光, 王刚, 王宗起, 武昱东, 王东升, 王嘉玮. 2018. 湖北武当山南缘房县地区早古生代镁铁质岩石成因及大地构造意义力学. 地球学报, 39(3): 306~318.

许志琴, 卢一伦, 汤耀庆, 张治洮. 1988. 东秦岭复合山链的形成: 变形、演化及板块动力学. 北京: 中国环境科学出版: 1~193.

许志琴, 李源, 梁凤华, 裴先治. 2015. "秦岭-大别-苏鲁"造山带中"古特提斯缝合带"的连接. 地质学报, 89(4): 671~680.

薛怀民, 马芳, 宋永勤. 2011. 扬子克拉通北缘随(州)-枣(阳)地区新元古代变质岩浆岩的地球化学和 SHRIMP 锆石 U-Pb 年代学研究. 岩石学报, 27(4): 1116~1130.

杨经绥, 许志琴, 马昌前, 吴才来, 张建新, 王宗起, 王国灿, 张宏飞, 董云鹏, 赖绍聪. 2010. 复合造山作用和中国中央造山带的科学问题. 中国地质, 37(1): 1~11.

杨佳林, 顾玉超, 杨凤超, 李东涛, 鞠楠, 贾宏翔. 2018. 辽东半岛大金山花岗岩体 SHRIMP U-Pb 年龄、元素地球化学和 Hf 同位素特征及地质意义. 地质论评, 64(6): 1541~1556.

赵国春, 胡健民, 孟庆任. 2003. 武当地块西部席状基性侵入岩群地球化学特征:南秦岭古生代底侵作用的依据. 岩石学报, 19(4): 612~622.

邹先武, 段其发, 汤朝阳, 曹亮, 崔森, 赵武强, 夏杰, 王磊. 2011. 北大巴山镇坪地区辉绿岩锆石 SHRIMP U-Pb 定年和岩石地球化学特征. 中国地质, 38(2): 282~291.

张成立, 高山, 张国伟, 柳小明, 于在平. 2002. 南秦岭早古生代碱性岩墙群的地球化学及其地质意义. 中国科学(D 辑), 32(10): 819~829.

周鼎武, 张成立, 王居里, 刘良, 董云鹏, 刘颖宇, 韩松. 1997. 武当地块基性岩墙群初步研究及其地质意义. 科学通报, 42(23): 2546~2549.

周鼎武, 张成立, 华洪, 胡建民. 1998. 南秦岭中、新元古代地层划分对比新认识. 高校地质学报, 4(3): 350~357.

周鼎武, 张成立, 周小虎, 桑海清. 1999. 武当地块基性岩墙群 $^{40}$Ar

/$^{39}$Ar 定年及其地质意义. 岩石学报, 15(1): 14~20.
张国伟. 1991. 试论秦岭造山带岩石圈构造演化基本特征. 西北地质, 21(2): 77~87.
张国伟, 张宗清, 董云鹏. 1995. 秦岭造山带主要岩石地层单元的构造性质及其大地构造意义. 岩石学报, 11(2): 101~104.
张国伟, 张本仁, 袁学诚. 2001. 秦岭造山带与大陆动力学. 北京: 科学出版社: 1~855.
张国伟, 郭安林, 董云鹏, 姚安平. 2019. 关于秦岭造山带. 地质力学学报, 25(5): 746~768.
张永清, 张健, 李怀坤, 陆松年. 2013. 南秦岭武当山群变质酸性火山岩锆石 U-Pb 年代学. 地质学报, 87(7): 922~930.
祝禧艳, 陈福坤, 王伟, Hieu P T, 王芳, 张福勤. 2008. 豫西地区秦岭造山带武当山群火山岩和沉积岩锆石 U-Pb 年龄. 科学通报, 29(6): 817~829.
祝禧艳, 陈福坤, 杨力, 王伟, Hieu P T, 苗来成, 张福勤. 2009. 豫西地区秦岭造山带武当群 Nd-Hf 同位素组成及其物源特征. 岩石学报, 25(11): 3017~3028.
Agrawal S, Guevara M, Verma S. 2008. Tectonic discrimination of basic and ultrabasic volcanic rocksthrough log - transformed ratios of immobile trace elements. International Geology Review, 50(12): 1057~1079.
Aldanmaz E, Pearce J A, Thirlwall M F, Mitchell J G. 2000. Petrogenetic evolution of late Cenozoic, post-collision volcanism in western Anatolia, Turkey. Journal of Volcanology and Geothermal Research, 10(1~2): 67~95.
Aldanmaz E, Köprübaşı N, Gürer Ö F, Kaymakçı N, Gourgaud A. 2006. Geochemical constraints on the Cenozoic, OIB-type alkaline volcanic rocks of NW Turkey: Implications for mantle sources and melting processes. Lithosphere, 86(1~2): 50~76.
Amelin Y, Lee D C, Alex N, Halliday, Robert T, Pidgeon. 1999. Nature of the earth's earliest crust from hafnium isotopes in single detrital zircons. Nature, 399: 252~255.
Bader T, Ratschbacher L, Franz L, Yang Z, Hofmann M, Linnemann U, Yuan H L. 2013. The heart of China revisited, I. Proterozoic tectonic of the Qin Mountain in the core of supercontinent Rodinia. Tectonics, 32: 661~687.
Barrett T J, Maclean W H. 1999. Volcanic sequences, lithogeochemistry, and hydrothermal alteration in some bimodal volcanic-associated massive sulfide systems. In: Barrie C T, et al. (Eds.), Volcanic-Associated Massive Sulfide Systems: Processes and Examples in Modern and Ancient Settings. Reviews in Economic Geology, 8: 101~131.
Blichert-Toft J, Albarède F. 1997. The Lu-Hf isotope geochemistry of chondrites and the evolution of the mantle-crust system. Earth and Planetary Science Letters, 148(1~2): 243~258.
Cai Zhiyong, Luo Hong, Xiong Xiaolin, Wu Dekuan, Wu Xianliang, Sun Sancai, Yang Jun. 2006&. A discussion on the age of the meta sedimentary rocks in the upper part of the Wudang Group constrained by the grain - zircon U - Pb dating. Journal of Stratigraphy, 30(1): 60~63.
Chen Jinbiao, Qin Zhengyong, Wang Shouqiong. 1991#. Geological Characteristics of the Wudang Group. Tianjin: Tianjin Science and Technology Publishing House: 1~130.
Choe W H, Lee J I, Lee M J, Mi J L, Hur S D, Jin Y K. 2007. Origin of E-MORB in a fossil spreading center: The Antarctic-Phoenix ridge, drake passage, Antarctica. Geosciences Journal, 11(3): 185~199.
Cole R B, Nelson S W, Layer P W, Oswald P J. 2006. Eocene volcanism above a depleted mantle slab window in southern Alaska. Geological Society of America Bulletin, 118(1~2): 140~158.
Deng Jinfu, Luo Zhaohua, Su Shangguo. 2004#. Petrogenesis, Tectonic Setting and Mineralization. Beijing: Geological Publishing House: 1~381.
Deng Jinfu, Liu Cui, Feng Yanfang, Xiao Qinghui, Di Yongjun, Su Shangguo, Zhao Guochun, Duan Peixin, Dai Meng. 2015. On the correct application in the common igneous petrological giagrams: Discussion and suggestion. Geological Review, 61(4): 717~734.
Dong Yunpeng, Zhang Guowei, Neubauer F, Liu Xiaoming, Genser J, Hauzenberger C. 2011. Tectonic evolution of the Qinlingorogen, China: Review and synthesis. Journal of Asian Earth Sciences, 41(3): 213~237.
Dong Yunpeng, Zhang Xiaoning, Liu Xiaoming, Li Wei, Chen Qing, Zhang Guowei, Zhang Hongfu, Yang Zhao, Sun Shengsi, Zhang Feifei. 2015. Propagation tectonics and multiple accretionary processes of the Qinling Orogen. Journal of Asian Earth Sciences, 104: 84~98.
Fu Jianming, Zhang Yeming, Cai Jinhui, Chen Shengfeng. 1999&. Original petrology and tectonic setting of meta volcanic rocks in Wudang Rock Group. Geological Review, 45(7): 668~673.
Furman T Y, Bryce J G, Karson J, Lotti A. 2004. East African rift system (EARS) Plume structure: insights from quaternary mafic lavas of Turkana, Kenya. Journal of Petrology, 45(5): 1069~1088.
Geng Hongyan, Sun Min, Yuan Chao, Xiao Wenjiao, Xian Weisheng, Zhao Guochun, Zhang Lifei, Wong Kenny, Wu Fuyuan. 2009. Geochemical, Sr-Nd and zircon U-Pb-Hf isotopic studies of late carboniferous magmatism in the West Junggar, Xinjiang: Implications for ridge subduction? Chemical Geology, 266(3~4): 364~389.
Greenough J D, Dostal J, Mallory-Greenough L M. 2005. Oceanic island volcanism II: mantle processes. Geoscience Canada, 32: 77~90.
Gribble R F, Stern R J, Bloomer S H. 1996. MORB mantle and subduction components interact togenerate basalts in the southern Mariana Trough back - are basin. Geochimica et Cosmochimica Acta, 60(12): 2153~2166.
Griffin W L, Pearson N J, Belousova E, Jackson S E, Achterbergh E, O'Reilly Suzanne Y, Shee S R. 2000. The Hf isotope composition of cratonic mantle: LAM-MC-ICPMS ananlysis of zircon megacrysts in kimberlites. Geochimica et Cosmochimica Acta, 64(1): 133~147.
Hawkins J W. 2003. Geology of supra-subduction zones: Implications for the origin of ophiolits. In: Dilek Y, Newcomb S (eds.). Ophiolite Concept and the Evolution of Geological Thought. Geological Society of America Special Paper, 373: 227~268.
Hemond C, Hofmann A W, Vlastlic I, Naurent F. 2006. Origin of MORB enrichment and relative trace element compatibilities along the Mid - Atlantic Ridge between 10° and 24° N. Geochemistry Geophysics Geosystems, 7 (12): Q12010. doi: 10. 1029/2006GC001317, ISSN: 1525~2027
Hess P C. 1992. Phase equilibria constraints on the origin of ocean floor basalts. In: Morgan J P, Blackman D K, Sinton J M (eds.). Mantle Flow and Melt Generation at Mid - Ocean Ridges. Geophysical Monograph, American Geophysical Union, 71: 67~102.
Hofmann A W, Jochum K P, Seufert M, White W M. 1986. Nb and Pb in oceanic basalts: new constraints on mantle evolution. Earth and Planetary Science Letters, 79: 33~45.
Hou Kejun, Li Yanhe, Tian Yourong. 2009&. In situ U-Pb zircon

dating using laser ablation－multi ion counting, LA－ICP－MS. Mineral Deposits, 28(4): 481~492.

Huang Daomao, Wan Yusheng, Zhang Dehui, Dong Chunyan, Zhao Yuanyi. 2016&. Paleoproterozoic tectono－thermal events in the Xiatang area, Lushan County, southern margin of the North China Craton－Evidence from geochemical features, zircon SHRIMP dating and Hf isotopic analysis. Geological Review, 62(6): 1439~1461.

Hu Jianmin, Meng Qingren, Ma Guoliang, Zhang Senqi, Gao Diansong. 2002&. Basic sill swarms in Wudang block of the Southern Qinling and its geological significance. Geological Review, 48(4): 353~360.

Hu Jianmin, Guo Liyu, Song Zixin, Li Xia, Liu Shoujun. 1995&. The contract relation of the Wudangshan Group and the Yaolinghe Group in the north margin of Yangzi massif and its significance. Journal of Xi'an College of Geology, 17(1): 22~27.

Hu Jianmin, Zhao Guochun, Meng Qingren, Luo Hong, Wang Zonghe. 2003&. The geological features and tectonic significances of the basic swarms in Wudang terrain of Qinling orogeny. Acta Petrologica Sinica, 19(4): 601~611.

Hu Jianmin, Zhao Guochun, Ma Guoliang, Zhang Senqi, Gao Diansong. 2004&. Paleozoic extensional tectonics of the Wudang block in the Qinling Orogen, China. Chinese Journal of Geology, 39(3): 305~319.

Keppler H. 1996. Constraints from partitioning experiments on the composition of subduction-zone fluids. Nature, 380(6571): 237~240.

Li Chunyu, Liu Yangwen, Zhu Baoqing. 1978#. Tectonic Evolution of the Qinling and Qilian Mountains. In: Contributions to 26th Internal Geological Congress, volume(1). Beijing: Geological Publishing House: 174~187.

Li Qiwei, Zhao Junhong. 2016. Petrogenesis of the Wudang mafic dikes: Implications of changing tectonic settings in South China during the Neoproterozoic. Precambrian Research, 272: 101~114.

Li Shuguang, Sun Weidong, Zhang Guowei, Chen Jiayi, Yang Yongcheng. 1996#. Chronology and geochemistry of metavolcanic rocks from Heigouxia valley in the Mian-Lue tectonic zone, South Qinling: Evidence for a Paleozoic oceanic basin and its close time. Science in China(Ser. D), 9(3): 300~310.

Li Sanzhong, Zhao Shujuan, Liu Xin, Cao Huahua, Yu Shan, Li Xiyao, Somerville Ian, Yu Shengyao, SuoYanhui. 2018. Closure of the Proto－Tethys Ocean and Early Paleozoic amalgamation of microcontinental blocks in East Asia. Earth Science Reviews, 186: 37~75.

Ling Wenli, Ren Bangfang, Duan Ruichun, Liu Xiaoming, Mao Xinwu, Peng Lianhong, Liu Zaoxue, Cheng Jianping, Yang Hongmei. 2007&. Timing of the Wudangshan, Yaolinghe volcanic sequences and mafic sills in South Qinling: U－Pb zircon geochronology and tectonic implication. Science Bulletin, 52(17): 1445~1456.

Liu Jiawei, Zhang Hongfu. 2018&. The petrogenesis and tectonic setting of the Neoproterozoic basic intrusions in the South Qinling orogenic belt: Constraints from the U-Pb geochronology and Hf-O isotopes. Journal of Northwest University(Natural Science Edition), 48(2): 268~283.

Ludwig K R. 2003. User´s manual for isoplot 3.0: Geochronological toolkit for Microsoft excel. Berkeley Geochronology Center Special Publication, 4: 1~70.

Metzger E, Miller R B, Harper G D. 2002. Geochemistry and tectonic setting of the ophiolitic ingalls complex, north cascades, Washington: Implications for correlations of jurassic cordilleran ophiolites. The Journal of Geology, 110(5): 543~560.

Middlemost Eric A K. 1994. Naming materials in the magma/igneous rock system. Earth-Science Reviews, 37(3~4): 215~224.

Nie Hu, Wan Xin, Zhang He, He Jianfeng, Hou Zhenhui, Siebel W, Chen Fukun. 2016. Ordovician and Triassic mafic dykes in the Wudangterran: Evidence for opening and closure of the South Qinling ocean basin, central China. Lithos, 266: 1~15.

Niu Yaoling, Collerson K D, Batiza R, Wendt J I, Regelous M. 1999. Origin of enriched-type mid-ocean ridge basalt at ridges far from mantle plumes: The East Pacific rise at 11° 20′ N. Journal of Geophysical Research, 104(B4): 7067~7087.

Niu Yaoling, Regelous M, Wendt I J, Batiza R, O'Hara M J. 2002. Geochemistry of near－EPR seamounts: importance of source vs. process and the origin of enriched mantle component. Earth and Planetary Science Letters, 199(3~4): 327~345.

Pearce J A, Cann J R. 1973. Tectonic setting of basic volcanic rocks determined using trace element analysis. Earth and Planetary Science Letters, 19(2): 290~300.

Pearce J A, Lippard S J, Roberts S. 1984. Characteristics and Tectonic Significance of Supra－Subduction Zone Ophiolites. Geological Society, London, Special Publications, 16(1): 77~94.

Pearce J A. 1996. Source and settings of granitic rocks. Episodes, 19: 120~125.

Pearce J A. 2008. Geochemical fingerprinting of oceanic basalts with applications to ophiolite classification and the search for Archean oceanic crust. Lithos, 100: 14~48.

Qin Jiangfeng, Lai Shaocong, Li Yongfei. 2013. Multi－stage granitic magmatism during exhumation of subducted continental lithosphere: Evidence from the Wulong pluton, South Qinling. Gondwana Research, 24(3~4): 1108~1126.

Ratschbacher L, Hacker B R, Calvert A, Webb L E, Grimmer J C, McWilliams M O, Ireland T, Dong Shuwen, Hu Jianmin. 2003. Tectonics of the Qinling(Central China) tectonostratigraphy, geochronology, and deformation history. Tectonophysics: International Journal of Geotectonics and the Geology and Physics of the Interior of the Earth, 366(1~2): 1~53.

Rickwood P C. 1989. Boundary lines within petrologic diagrams which use oxides of major and minor elements. Lithos, 22(4): 247~263.

Riley T R, Leat P T, Pankhurst R J, Harris C. 2001. Origins of large volume rhyolitic volcanism in the Antarctic Peninsula and Patagonia crustal melting. Journal of Petrology, 42(6): 1043~1065.

Song Biao, Zhang Yuhai, Wan Yusheng. 2002&. Mount making and procedure of the SHRIMP dating. Geological Review, 48(suppl.): 26~30.

Sö derlund U, Patchett P J, Vervoort J D, Isachsen C E. 2004. The $^{176}$Lu decay constant determined by Lu－Hf and U－Pb isotope systematics of Precambrian mafic intrusions. Earth and Planetary Science Letters, 219(3~4): 311~324.

Su Wen, Liu Jingbo, Chen Nengsong, Guo Shun, Ba Jin, Zhang Lu, Liu Xin, Shi Yuxin. 2013&. Geochronology and tectonic background of magmatic and metamorphic events in the East Qinling-Dabie Mountains. Acta Petrologica Sinica, 29(5): 1573~1593.

Sun S S and McDonough W F. 1989. Chemical and isotopic systematics of oceanic basalts: Implications for mantle composition and processes. In: Saunders A D, Norry M J. eds. Magmatism in the Ocean Basins. Geological Society Special Publication, 42: 313~345.

Wang Cunzhi, Yang Kunguang, Xu Yang, Cheng Wanqiang. 2009&. Geochemistry and LA－ICP－MS zircon U－Pb age of asic dike swarms in north DABA mountains and its tectonic significance.

Geological Science and Technology Information, 28(3): 19~26.

Wang Dongsheng, Wang Zongqi, Wang Gang, Wu Yudong, Yang Hao. 2019&. Metamorphism of rocks in Shiyan-Wudang area of South Qinling tectonic belt, China. Journal of Earth Sciences and Environment, 41(9): 379~395.

Wang Gang, Wang Zongqi, Zhang Yingli, Wang Kunming, Wu Yudong. 2017. Devonian alkaline magmatism in South Qinling, China: evidence from the Taohekou Formation, Northern Daba Mountain. International Geology Review, 59(14): 1737~1763.

Wang Gang, Wang Zongqi, Wu Yudong, Wang Dongsheng, Wang Tao, Wang Jiawei, Zhang Hang. 2018&. The discovery of Late Paleozoic volcanic and sedimentary substances in the hinterland of Wudang Mountain, South Qinling Orogeny: Constrains from microfossil and zircon geochronology. Acta Geologica Sinica, 92(6): 1163~1175.

Wang Gang, Zhang Han, Wang Zongqi, Wu Yudong, Wang Dongsheng, Wang Jiawei. 2019&. Identification of the Permian E-MORB type basalts and their tectonic significance from Shiyan area, Wudang Mountain. Geological Review, 65(1): 65~84.

Wang Kunming, Wang Zongqi, Zhang Yingli, Wang Gang. 2014&. Mineral chemistry characteristics and indication significance of clinopyroxene in mafic rock of Gaoqiao area, North Daba Mountains. Acta Petrologica et Mineralogica, 33(3): 527~539.

Wang Kunming, Wang Zongqi, Zhang Yingli, Wang Gang. 2015. Geochronology and geochemistry of mafic rocks in the Xuhe, Shaanxi, China: Implications for petrogenesis and mantle dynamics. Acta Geologica Sinica(English edition), 89(1): 187~202.

Wang Lijuan, Griffin W L, Yu Jinhai, O'Reilly S Y. 2013. U-Pb and Lu-Hf isotopes in detrital zircon from Neoproterozoic sedimentary rocks in the northern Yangtze Block. Gondwana Research, 23(4): 1261~1272.

Wang Ruirui, Xu Zhiqin, Santosh M, Yao Yuan, Gao Lie, Liu Chunhua. 2016. Late neoproterozoic magmatism in South Qinling, central China: Geochemistry, zircon U-Pb-Lu-Hf isotopes and tectonic implications. Tectonophysic, 683: 43~61.

Wang Quan, Liu Xueya. 2010&. Is magmatic intrusion or exotic block emplacement? Geological Review, 56(3): 329~338.

Wang Tao, Wang Zongqi, Yan Quanren, Yan Zhen, Qin Xiaofeng, Zhang Yingli, Xiang Zhongjin. 2011&. The formation age and geochemical characteristics of the metavolcanic rock blocks of the Baishuijiang Group in South Qinling. Acta Petrologica Sinica, 27(3): 645~656.

Wang Zongqi, Yan Quanren, Yan Zhen, Wang Tao, Jiang Chunfa, Gao Lianda, Li Qiugen, Chen Junlu, Zhang Yingli, Liu Ping, Xie Chunlin, Xiang Zhongjin. 2009&. New division of the main tectonic units of the Qinling orogenic belt, Central China. Acta Geologica Sinica, 83(11): 1527~1546.

Wu Fuyuan, Li Xianhua, Zheng Yongfei, Gao shan. 2007&. Lu-Hf isotopic systematics and their application in petrology. Acta Petrologica Sinica, 23(2): 185~220.

Xu Guang, Wang Gang, Wang Zongqi, Wu Yudong, Wang Dongsheng, Wang Jiawei. 2018&. Petrogenesis of the Early Paleozoic mafic rock in Fangxian Area on the Southern Margin of Wudang Mountain, Hubei Province, and its tectonic significance. Acta Geoscientica Sinica, 39(3): 306~318.

Xu Yang, Yang Kunguang, Polat A, Yang Zhenning. 2016. The 860 Ma mafic dikes and granitoids from the northern margin of the Yangtze Block, China: A record of oceanic subduction in the early Neoproterozoic. Precambrian Research, 275: 310~331.

Xu Zhiqin, Luo Yilun, Tang Yaoqing, Zhang Zhitao. 1988&. Formation of the Composite Eastern Qinling chains. Beijing: Environmental Science Press: 1~193.

Xu Zhiqin, Li Yuan, Liang Fenghua, Pei Xianzhi. 2015&. A connection between the Paleo-Tehtys suture zone in the Qinling-Dabie-Sulu orogenic belt. Acta Geologica Sinica, 89(4): 671~680.

Xue HuaiMin, Ma Fang, Song Yongqin. 2011&. Geochemistry and SHRIMP zircon U-Pb data of Neoproterozoic meta-magmatic rocks in the Suizhou-Zaoyang area, northern margin of the Yangtze craton, central China. Acta Petrologica Sinica, 27(4): 1116~1130.

Yan Zhen, Wang Zongqi, Yan Quanren, Wang Tao, Guo Xianqing. 2012. Geochemical constraints on the provenance and depositional setting of the Devonian Liuling Group, east Qinling Mountains, central China: Implication for the tectonic evolution of the Qinling orogenic belt. Journal of Sedimentary Research, 82: 9~20.

Yang Jingsui, XU Zhiqin, Ma Changqian, Wu Cailai, Zhang Jianxin, Wang Zhongqi, Wang Guocan, Zhang Hongfei, Dong Yunpeng, Lai Shaocong. 2010&. Compound orogeny and scientific problems concerning the central orogenic belt of China. Geology in China, 37(1): 1~11.

Yang Jialin, Gu Yuchao, Yang Fengchao, Li Dongtao, Ju Nan, Jia Hongxiang. 2018&. SHRIMP U-Pb ages, elements geochemistry and Hf isotopic characteristics of the Dajinshan granite in Liaodong Peninsula and geological significance. Geological Review, 64(6): 1541~1556.

Zou Xianwu, Duan Qifa, Tang Chaoyang, Cao Liang, Cui Sen, Zhao Wuqiang, Xia Jie, Wang Lei. 2011&. SHRIMP zircon U-Pb dating and lithogeochemical characteristics of diabase from Zhenping area in north Daba Mountain. Geology in China, 38(2): 282~291.

Zhao Guochun, Hu Jianmin, Meng Qingren. 2003&. Geochemistry of the basic sills in the western Wudang block: the evidences of the Paleozoic underplating in South Qinling. Acta Petrologica Sinica, 19(4): 612~622.

Zhang Chengli, Gao Shan, Zhang Guowei, Liu Xiaoming, Yu Zaiping. 2002&. Geochemistry of the Early Paleozoic alkali dikes in South Qinling, and geological implication. Science in China (Ser. D), 32(10): 819~829.

Zhang Guowei. 1991&. A discussion on basic features of tectonic development of lithosphere of the Qinling belt. Journal of Northwest University, 21(2): 77~87.

Zhang Guowei, Zhang Zongqi, Dong Yunpeng. 1995&. Nature of main tectono-lithostratigraphic units of the Qinling orogeny: Implication or the tectonic evolution. Acta Petrologica Sinica, 11(2): 101~104.

Zhang Guowei, Zhang Benren, Yuan Xuecheng. 2001&. Qinling Orogenic Belt and Continental Dynamics. Beijing: Science Press: 1~855.

Zhang Guowei, Guo Anlin, Dong Yunpeng, Yao Anping. 2019&. Rethinking of the Qinling orogeny. Journal of Geomechanics, 25(5): 746~768.

Zhang Yongqing, Zhang Jian, Li Huaikun, Lu Songnian. 2013&. Zircon U-Pb geochronology of the meta-acidic volcanic rocks from the Wudangshan Group, Southern Qinling Mountains, central China. Acta Geologica Sinica, 87(7): 922~930.

Zhou Dingwu, Zhang Chengli, Wang Juli, Liu Liang, Dong Yunpeng, Liu Yingyu, Han Song. 1997&. Study on mafic dikes within the Wudang Group and their geological significance. Chinese Science Bulletin, 42(23): 2546~2549.

Zhou Dingwu, Zhang Chengli, Hua Hong, Hu Jianmin. 1998&. New

knowledge about division and correlation of the Mid- and Neo-Proterozoic strata in the South Qinling. Geological Journal of China Universities, 4(3): 350~357.

Zhou Dingwu, Zhang Chengli, Zhou Xiaohu, Sang Haiqing. 1999&. $^{40}Ar/^{39}Ar$ dating of basic dykes from Wudang block and their geology significance. Acta Petrologica Sinica, 15(1): 14~20.

Zhu Xiyan, Chen Fukun, Wang Wei, HIEU P T, Wang Fang, Zhang Fuqin. 2008#. Zircon U-Pb ages of volcanic and sedimentary rocks of the Wudang Group in the Qinling orogenic belt within western Henan province. Acta Geoscientica Sinica, 29(6): 817~829.

Zhu Xiyan, Chen Fukun, Yang Li, Wang Wei, HIEU P T, Miao Laicheng, Zhang Fuqin. 2009&. Zircon Hf istopic composition and source characteristics of the Wudang Group in the Qingling orogenic belt, western Henan Province. Acta Petrologica Sinica, 25(11): 3017~3028.

Zhu Xiyan, Chen Fukun, Liu Bingxiang, Zhang He, Zhai Mingguo. 2015. Geochemistry and zircon ages of mafic dikes in the South Qinling, central China evidence for late neoproterozoic continental rifting in the northern Yangtze block. International Journal of Earth Sciences, 104: 27~44.

# Genesis and tectonic significance of Mesozoic mafic rocks in the Wudang Mountain-Shiyan Belt, South Qinling Orogen: Constraints from geochemistry and zircon U-Pb, Hf isotopes

WANG Jiawei[1,2)], WANG Gang[2)], WANG Zongqi[2)], WU Yudong[2)], WANG Dongsheng[2)], WANG Kunming[2)]

1) *China University of Geosciences(Beijing), Beijing*, 100083;

2) *MLR Key Laboratory of Metallogeny and Mineral Assessment, Institute of Mineral Resources, Chinese Academy of Geological Sciences, Beijing*, 100037

**Abstract**: Large-scale mafic dikes are developed in Northern Daba Mountain-Wudang Mountain- Shiyan and Suizhou areas of the South Qinling Orogen. Their petrogenesis and tectonic evolution are widely of interst to geologists. In this paper, whole-rock geochemistry, SHRIMP zircon U-Pb age and the LA-MC-ICP-MS zircon Hf isotopic compositions are used to study the gabbro occurring in the Huanglong-fangtan area of Wudang Mountain. The result indicates that these gabbros intruded during the Late Triassic (221.2 ±2.5 Ma); whole-rock geochemical data shows that the gabbros are sub-alkaline tholeiitic series with moderate concentrations of Ti, Zr, Hf and Nb, while exhibiting depletions of the large ion lithophile elements (LILE) such as Rb and Sr. The rare earth element (REE) distribution patterns display negative slopes with slight light rare earth element (LREE) enrichment and depletion of heavy rare earth elements (HREE), which are similar to that of enriched mid-ocean ridge basalt (E-MORB). The $\varepsilon_{Hf}(t)$ value of magmatic zircons are between -13.5 and -6.18 with ancient two-stage Hf model ages (2103~1640 Ma). In addition, the gabbros appear to have all originated from low-pressure and medium degree of partial melting of spinel lherzolite. The regional tectonic evolution combined with the new evidence for mantle enrichment, and the E-MORB affinities of the gabbros in this paper, suggests that these rocks formed in a convergent tectonic setting, affected by subduction of the Mianlue Ocean basin, and may thus be the product of the subduction-collisional stage.

**Keywords**: petrogenesis; Mesozoic; gabbro; Wudang Mountain; south Qinling Orogen

**Acknowledgements**: This study is supported by the National Key R & D Program of China (No. 2016YFC0600202) and Chinese Academy of Geological Sciences Research Fund (No. YK1701).

**First author**: WANG Jiawei, male, born in 1989, associated researcher, mainly engaged in the petrology and metallogeny research. Email: wangjiawei0824@163.com

**Corresponding author**: WANG Gang, male, born in 1984, doctor, associated researcher, mainly engaged in the tectonics and metallogeny research; Email: wanggang0315@126.com

**Manuscript** received on: 2021-01-15; Acceptedon: 2021-03-25; Network published on: 2021-05-20

**Doi**: 10.16509/j.georeview.2021.03.257　　**Edited by**: HUANG Daomao, LIU Zhiqiang